INTRODUCTION to ION BEAM TECHNIQUES

Marko Karlušić
Ruđer Bošković Institute, Zagreb

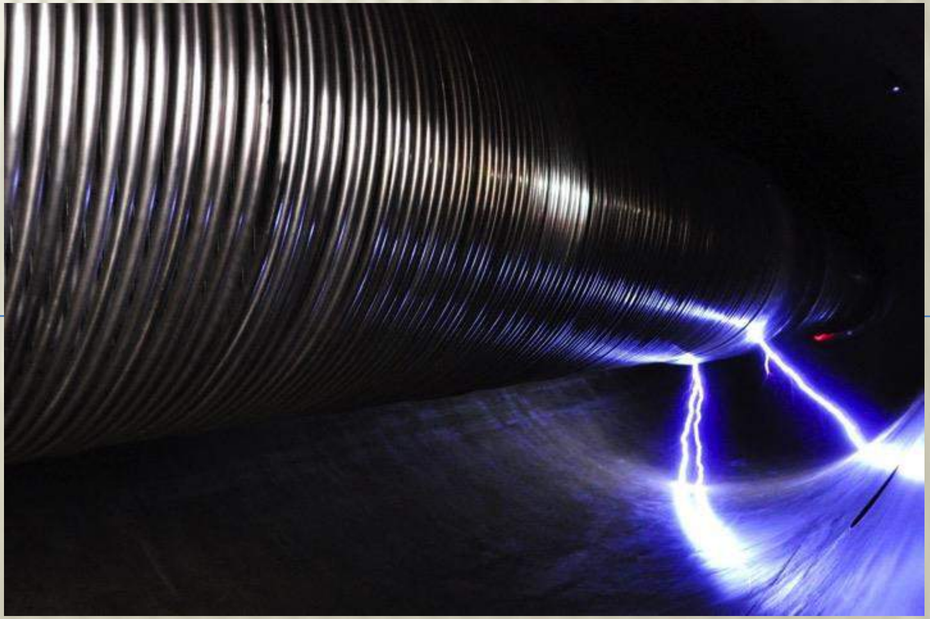

INTRODUCTION to ION BEAM ANALYSIS (IBA) TECHNIQUES (a.k.a. NUCLEAR ANALYTICAL METHODS)

- Electrostatic accelerators
- Ion beam analysis with examples
  - RBS
  - ERDA
  - PIXE
  - Nuclear microprobe
- Materials modification

Marko Karlušić
Ruđer Bošković Institute, Zagreb

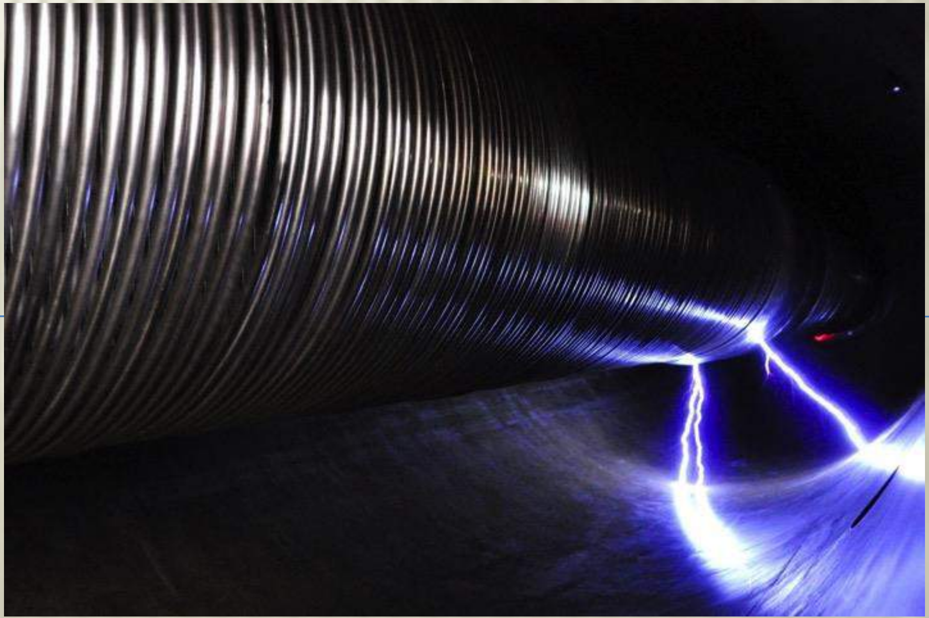

ELECTROSTATIC ACCELERATORS

The first ion probe – Rutherford experiment

Plum Pudding Model
of Atomic Structure

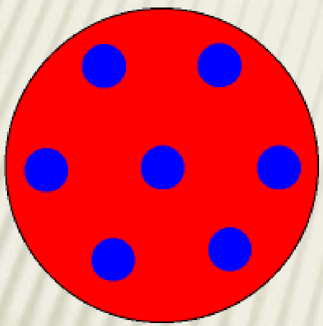

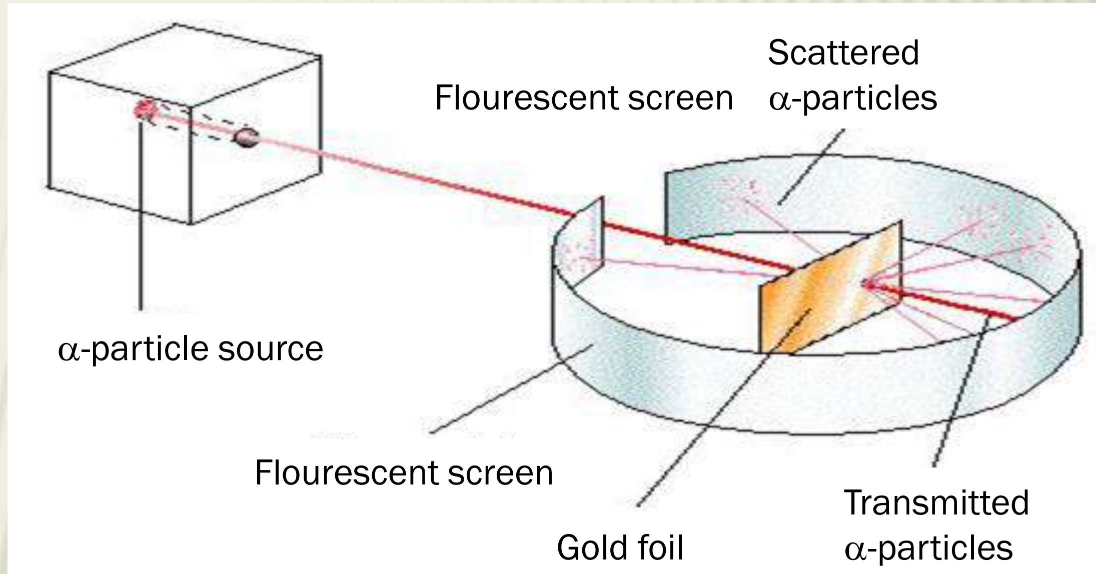

ERNEST RUTHERFORD

- 1909 – α-particle scattering experiment on gold foil
- 1911 – theory of nuclear atom
- had called for *"a million volts in a soapbox"* to advance nuclear research!

ELECTROSTATIC ACCELERATORS

Cockroft and Walton

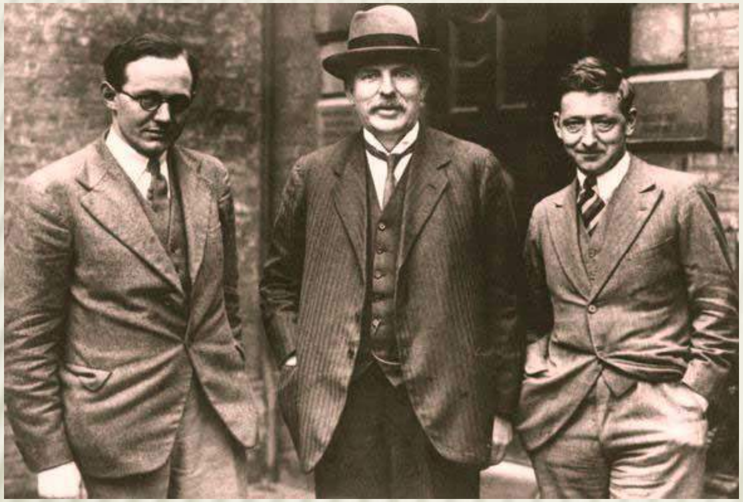

John Cockroft, sir Ernest Rutherford and Ernest Walton

Working in a vacant room at Rutherford's Cavendish Laboratory at Cambridge University, Englishman Cockcroft and Irishman Walton used spare parts to build the world's first nuclear-particle accelerator in 1929

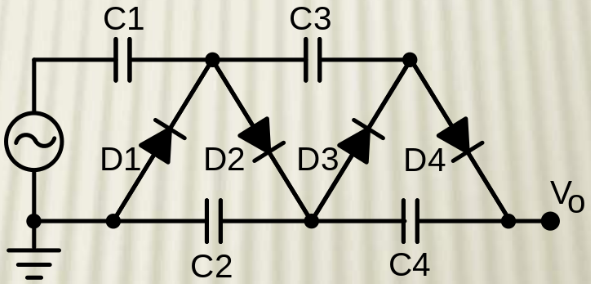

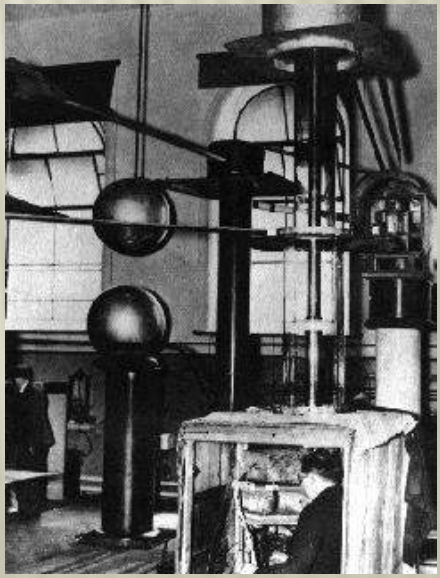

- high voltage obtained by cascade voltage multiplier
- 1932 the first artificial nuclear reaction $p+Li^7 \rightarrow He^4+He^4$
- Nobel prize 1951

ELECTROSTATIC ACCELERATORS

Robert J. Van de Graaff

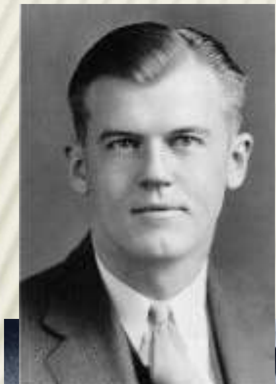

Princeton University; MIT Boston

- 1929 80 kV
- 1931 7 MV
- after the WWII he founded HVEC – High Voltage Engineering Corporation

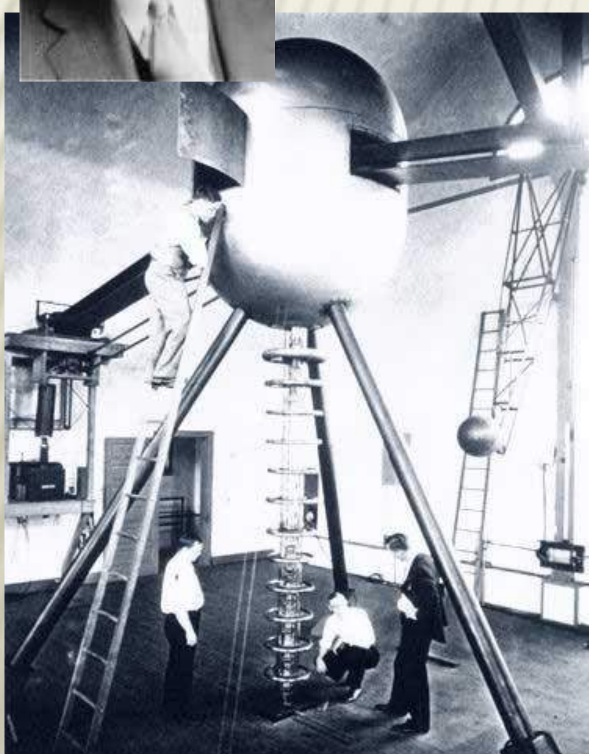

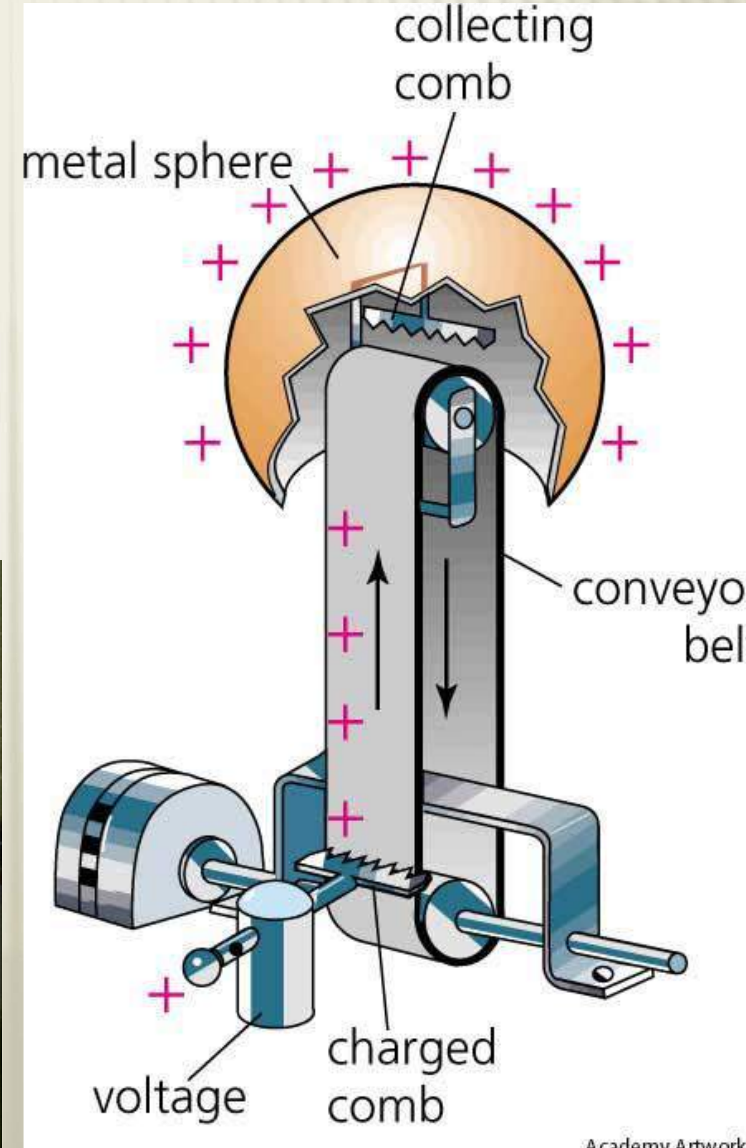

ELECTROSTATIC ACCELERATORS

Luis W. Alvares

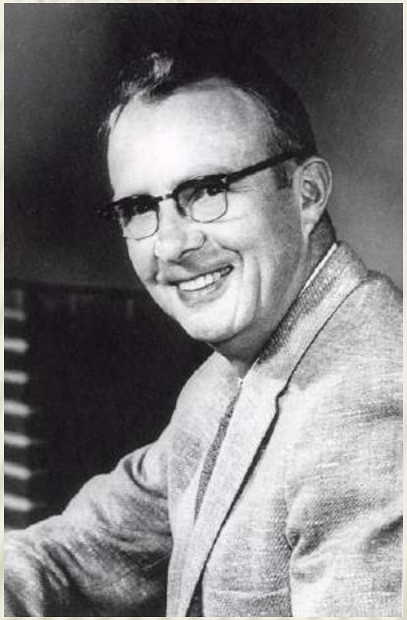

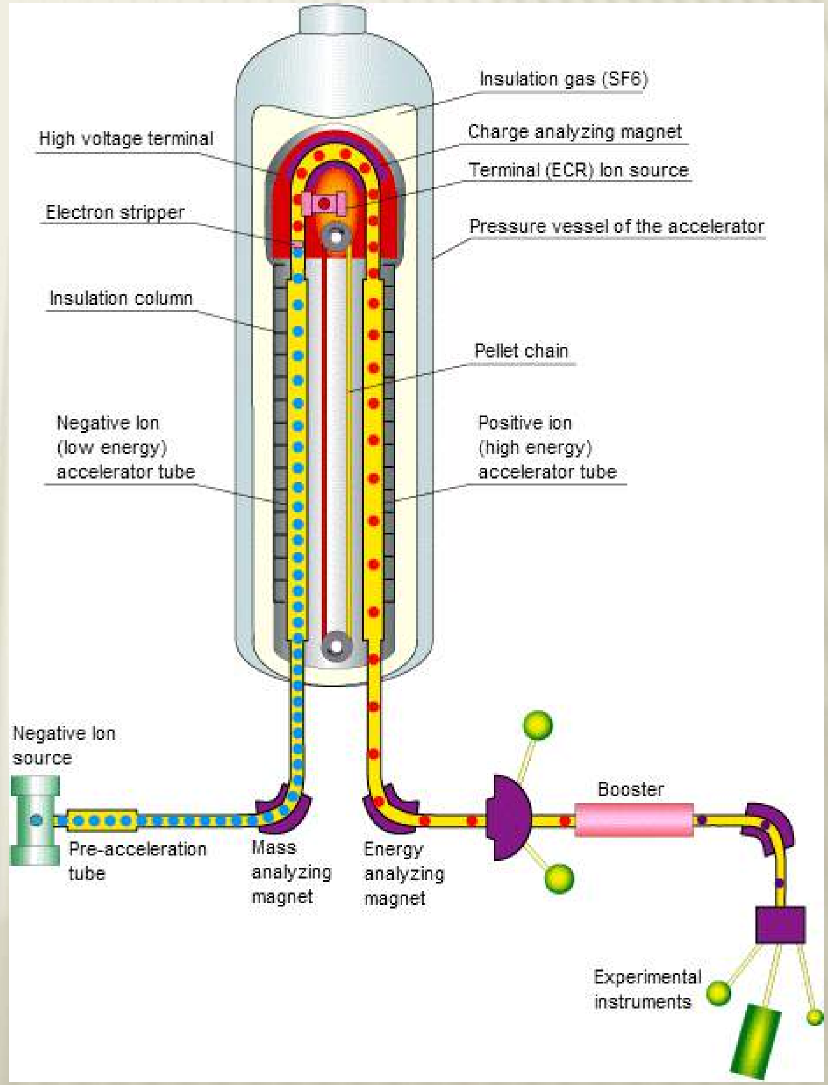

- WWII – Manhattan project
- Berkeley 1951 – concept of tandem accelerator
- Nobel prize in physics 1968 (bubble chamber)
- Alvarez Hypothesis 1980

ACCELERATORS TODAY

Aprox. 20.000 accelerators:

- 90% medicine & industry
  - Medicine
    - Diagnostics (isotope production)
    - Radiation treatment
  - Industry
    - Ion implanters
    - Electron accelerators for radiation processing (e.g. polimer crosslinking, sterilisation...)
- 10% research and education
  - Large scale facilities (e.g.CERN, GSI, etc.)
  - Synchrotron light sources
  - Cyclotrons
  - Electrostatic accelerators (including implanters)

ELECTROSTATIC ACCELERATORS

RBI-AF, Zagreb, Croatia

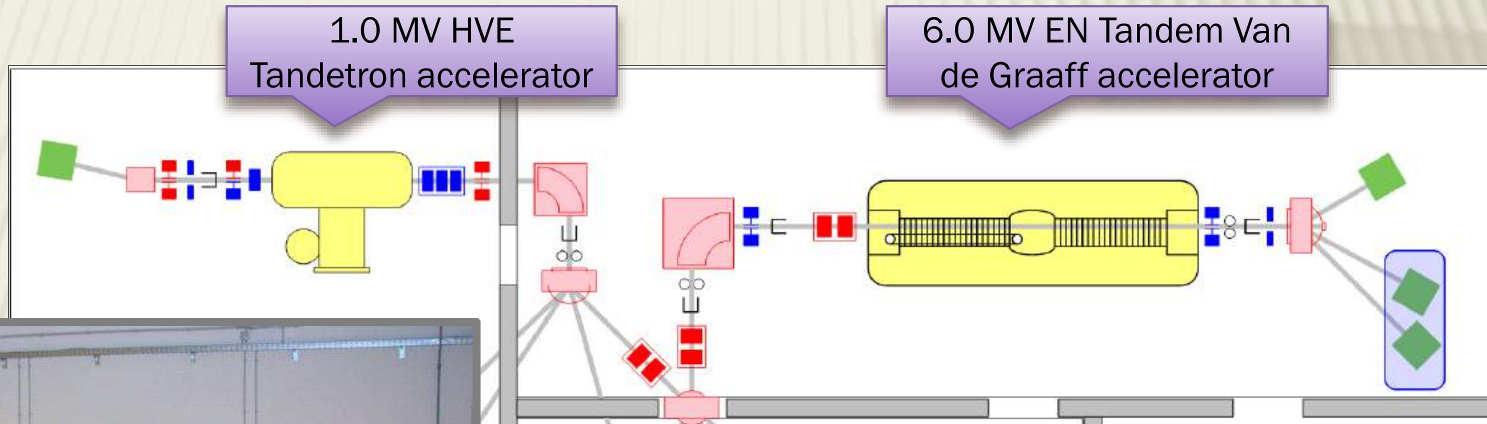

- 100 keV – 40 MeV
- p, He, Li, C, O, Si, Cl, I, Au….

RBI-AF, Zagreb, Croatia

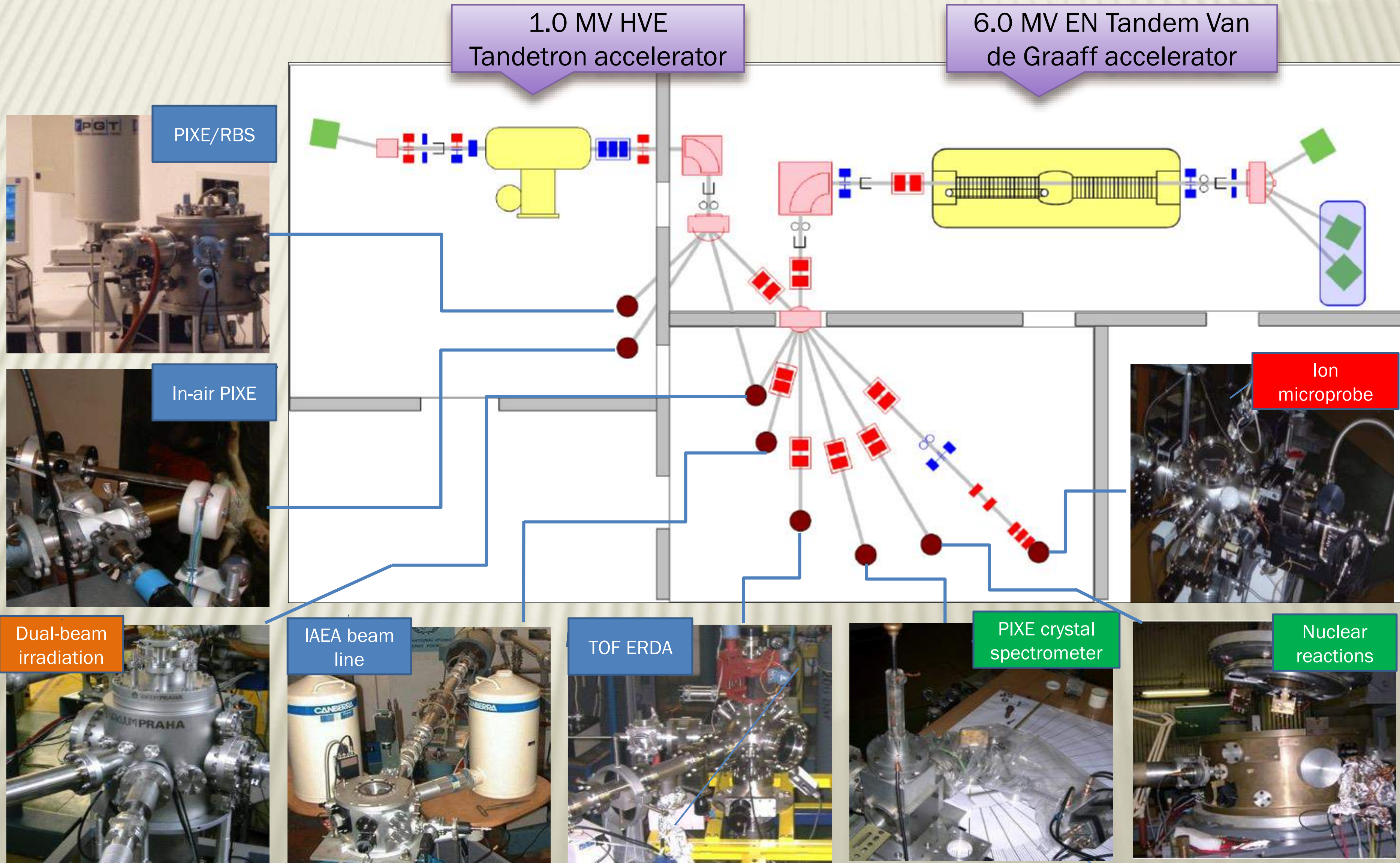

ION BEAM ANALYSIS

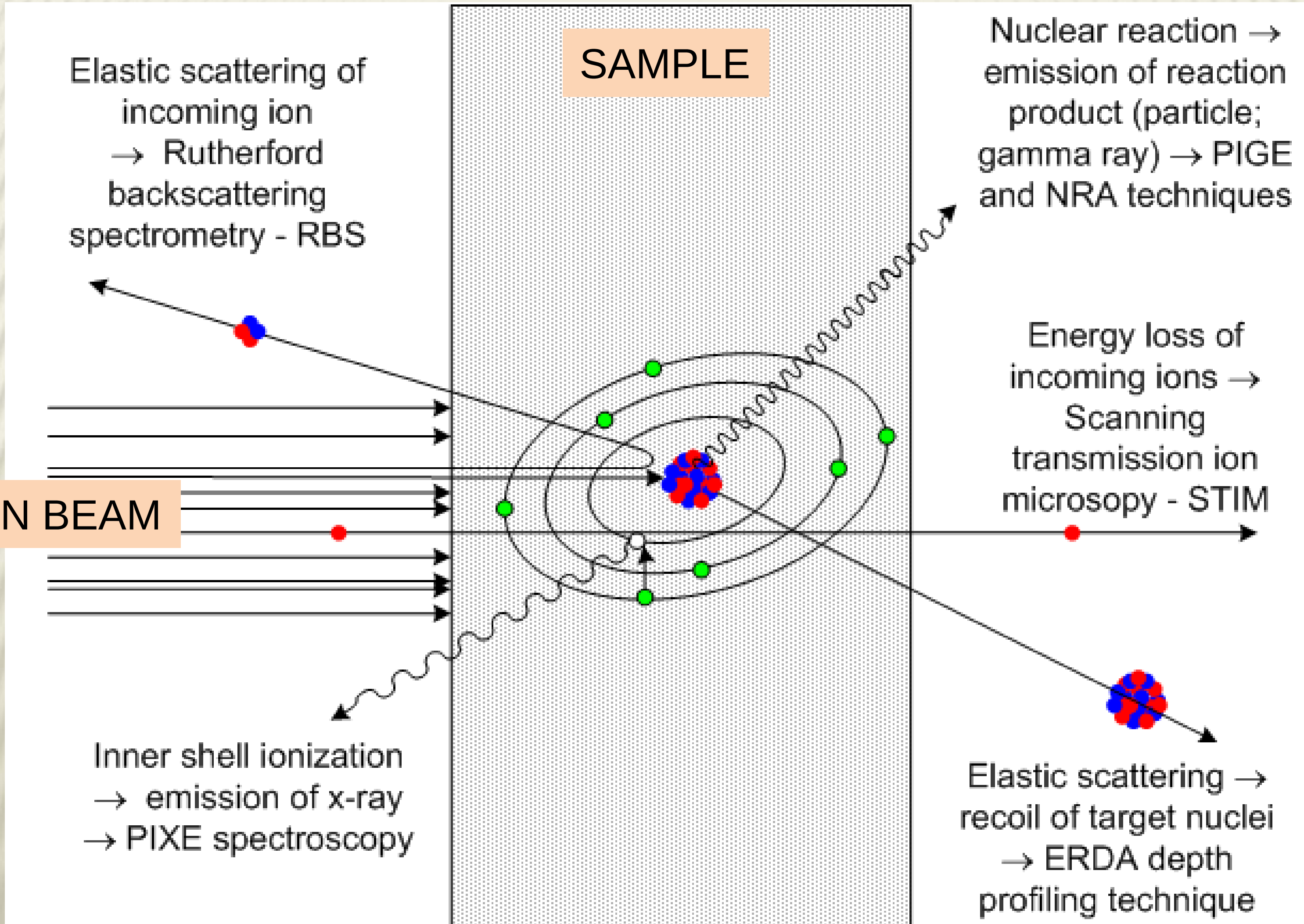

ION BEAM ANALYSIS

Non-destructive techniques (most of the time…)

1 BARN (b) = 100 fm^2

1 fm = 10^{-15} m

typical size of the nucleus

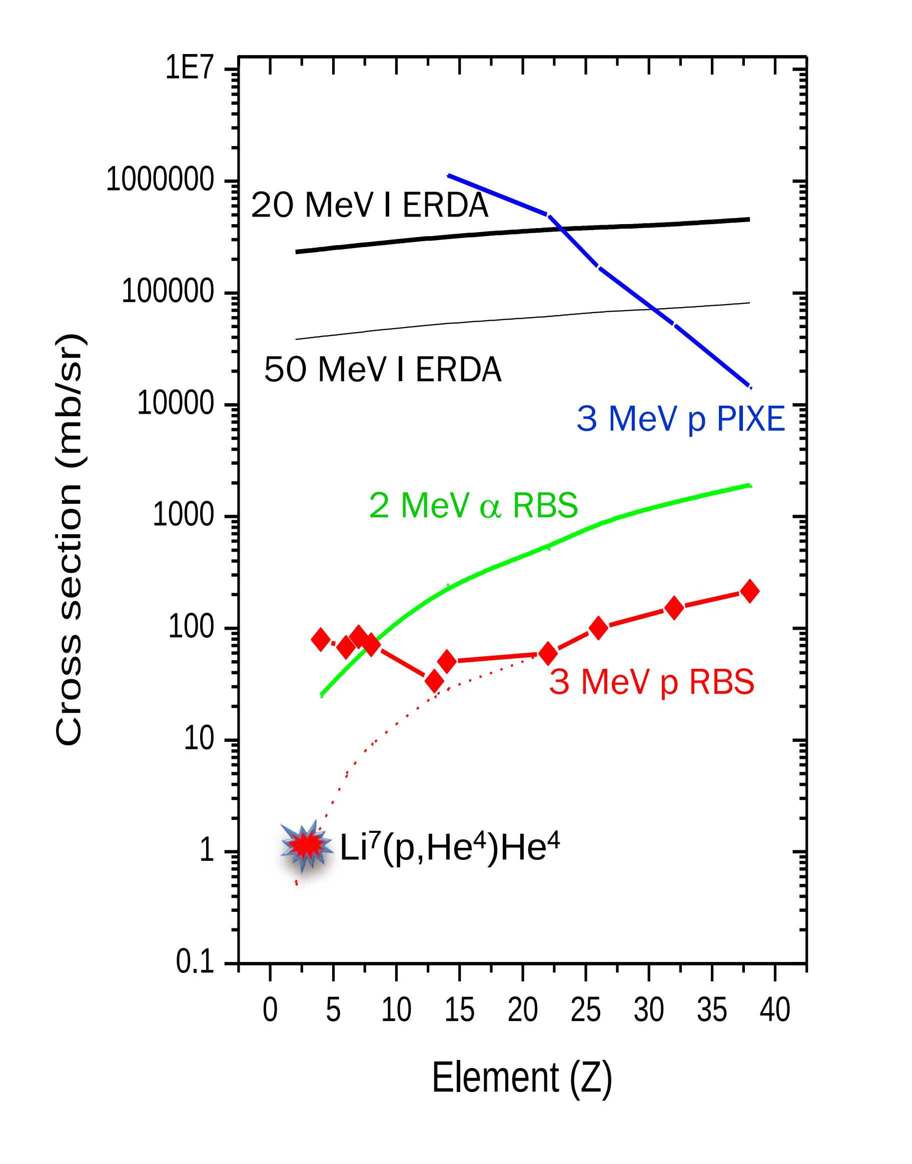

RUTHERFORD BACKSCATTERING SPECTROMETRY

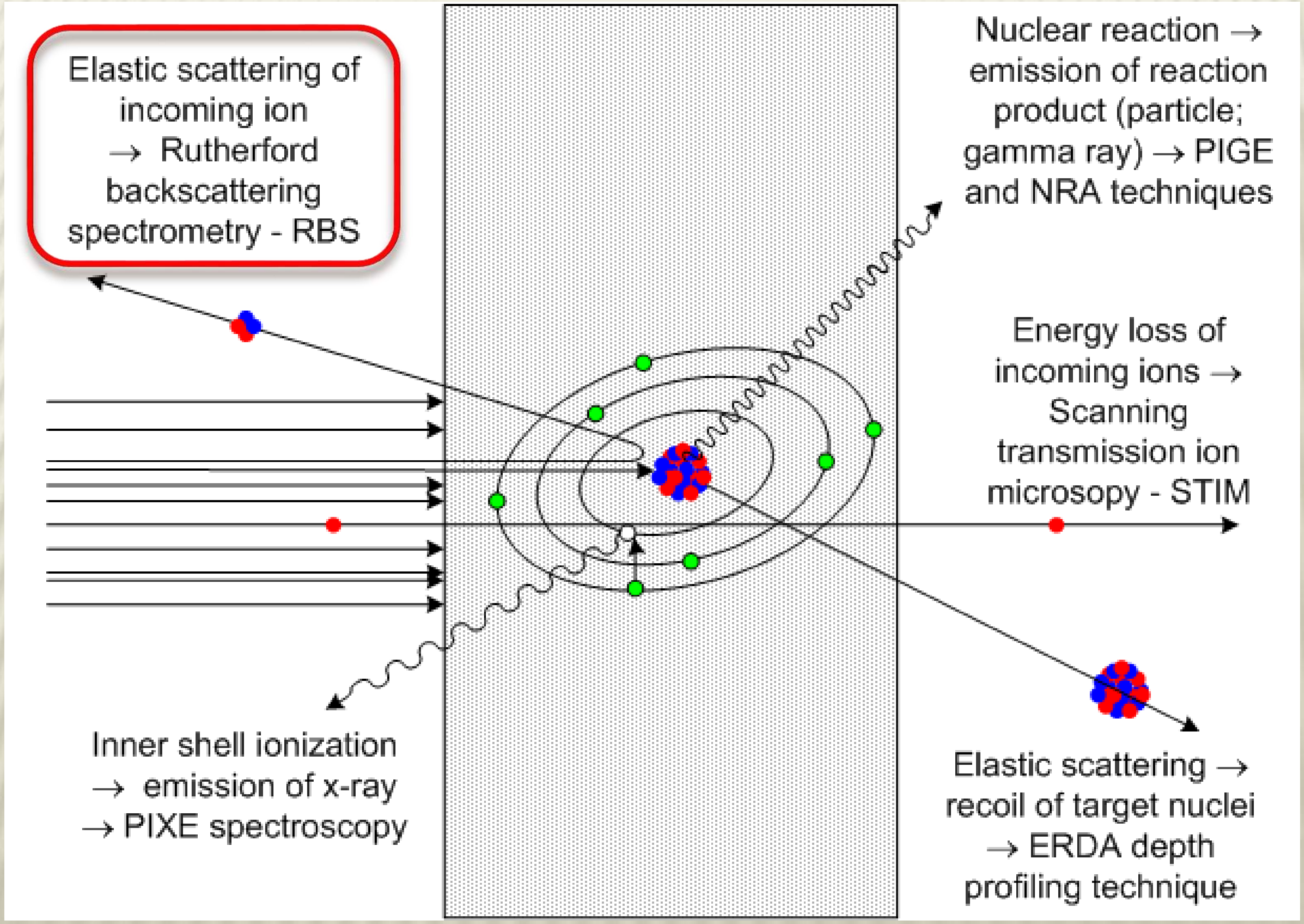

RUTHERFORD BACKSCATTERING SPECTROMETRY

$$K = \frac{E_{scattered}}{E_{incident}} = \left[\frac{\left(1 - \left(\frac{M_1 \sin\theta}{M_2}\right)^2\right)^{1/2} + \frac{M_1 \cos\theta}{M_2}}{1 + \frac{M_1}{M_2}} \right]^2$$

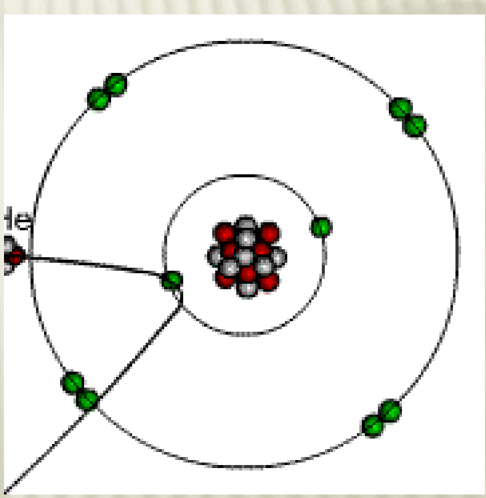

E	*Ion energy*
M_1	*Mass of incident ion*
M_2	*Mass of t arget atom*
θ	*Scattering angle*

For a given scattering angle Θ, known projectile energy $E_{inc.}$ and mass M_1 (eg. 2 MeV α), $E_{sc.}$ Can be measured and therefore unknown mass M_2 can be determined

RUTHERFORD BACKSCATTERING SPECTROMETRY

cross section

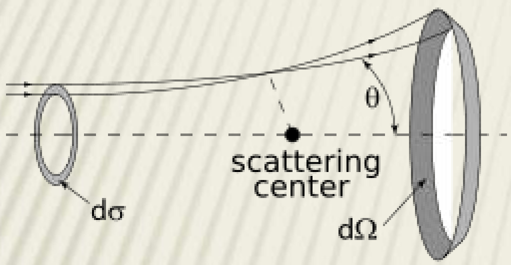

$$\frac{\partial\sigma}{\partial\Omega} = \left[\frac{Z_1 Z_2 e^2}{4E}\right]^2 \bullet \frac{4}{\sin^4\theta} \bullet \frac{\left[\sqrt{1-\left[\frac{M_1 \sin\theta}{M_2}\right]^2} + \cos\theta\right]^2}{\sqrt{1-\left[\frac{M_1 \sin\theta}{M_2}\right]^2}}$$

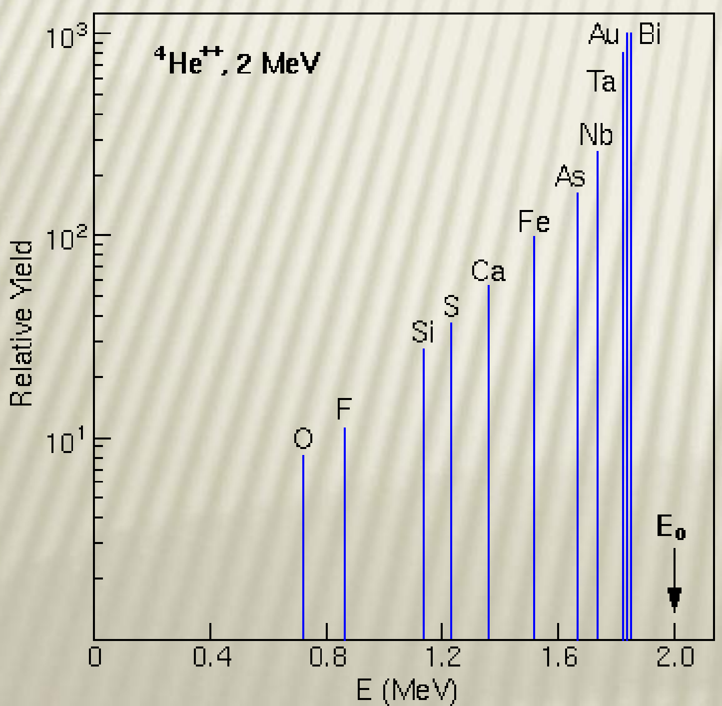

Z_1	Atomic number of incident ion
Z_2	Atomic number of target atom
E	Energy of incident ion
M_1	Mass of incident ion
M_2	Mass of target atom
θ	Angle of incidence

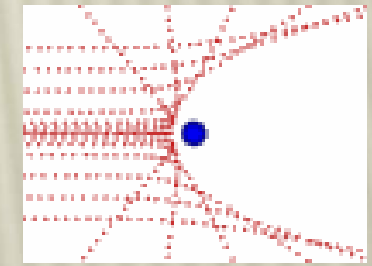

RUTHERFORD BACKSCATTERING SPECTROMETRY

DEPTH PROFILING

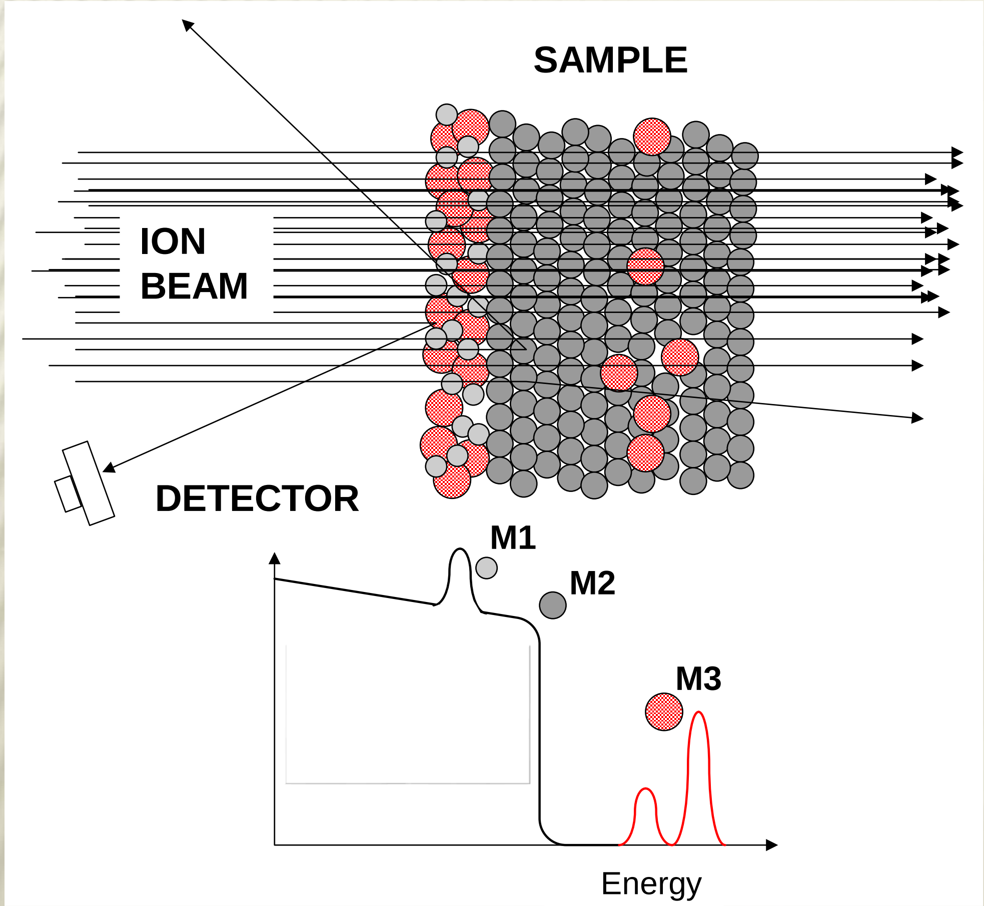

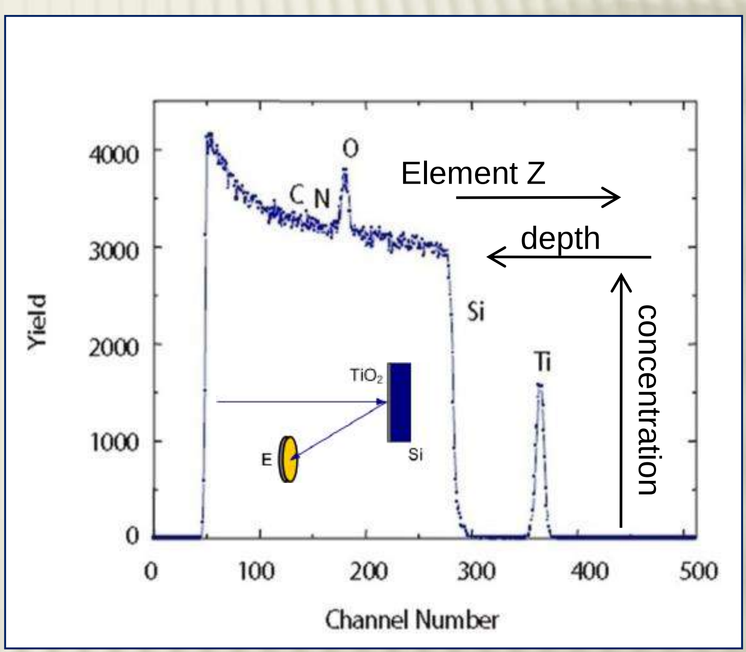

Proton beam (2 MeV)
Detector positioned at $\Theta=165^0$,

Sample: thin TiO_2 film on Si substrate

RUTHERFORD BACKSCATTERING SPECTROMETRY

DEPTH PROFILING

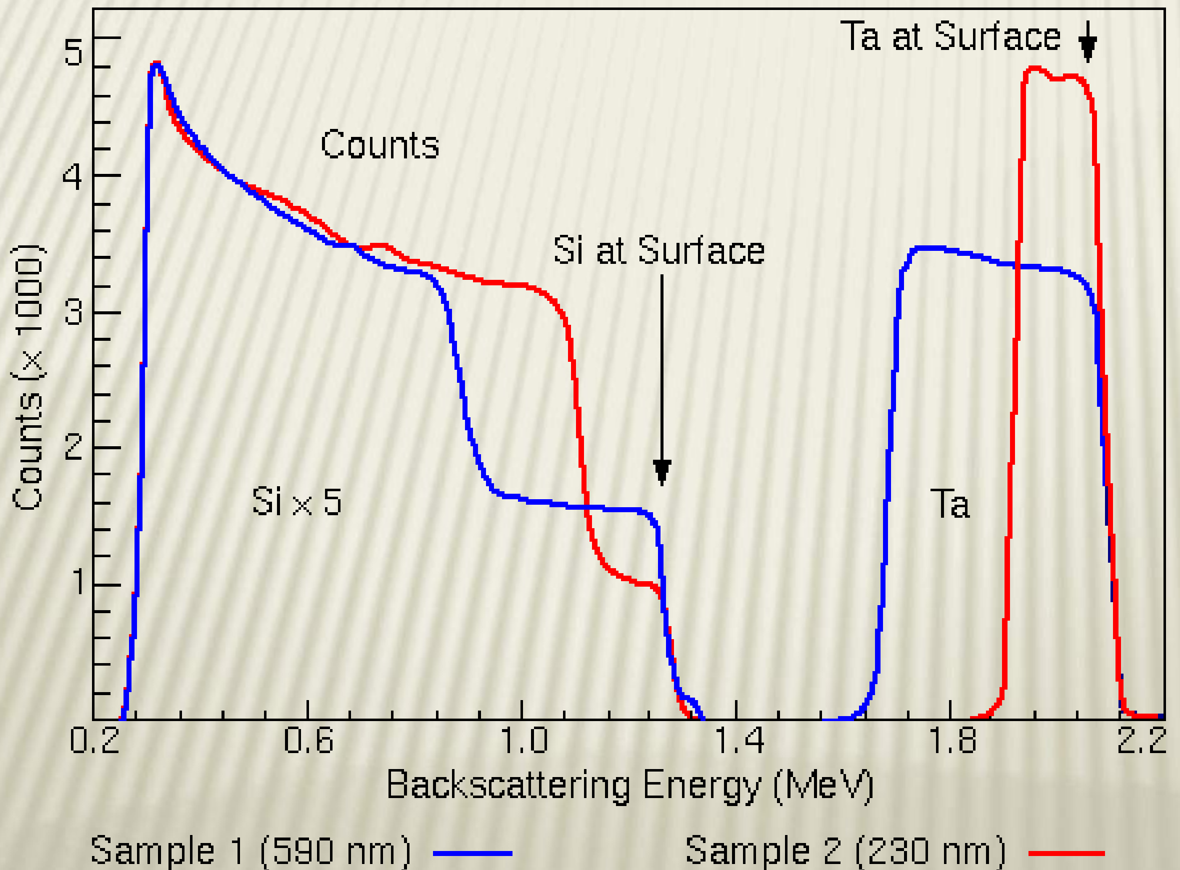

TaSi layers of 590 and 230 nm deposited on Si substrate as seen by 2 MeV alpha RBS

RBS –EXAMPLES

Sample:
thin film a-Si solar cell
(amorphous silicon)

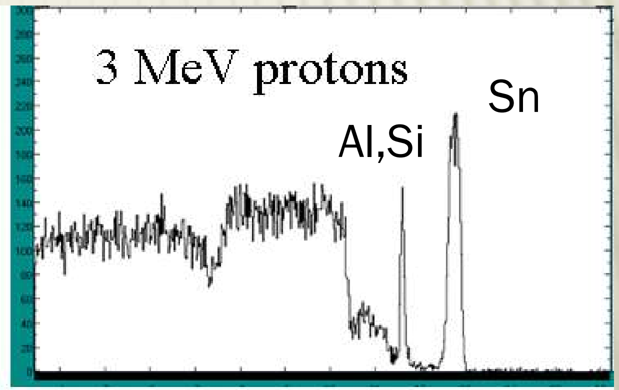

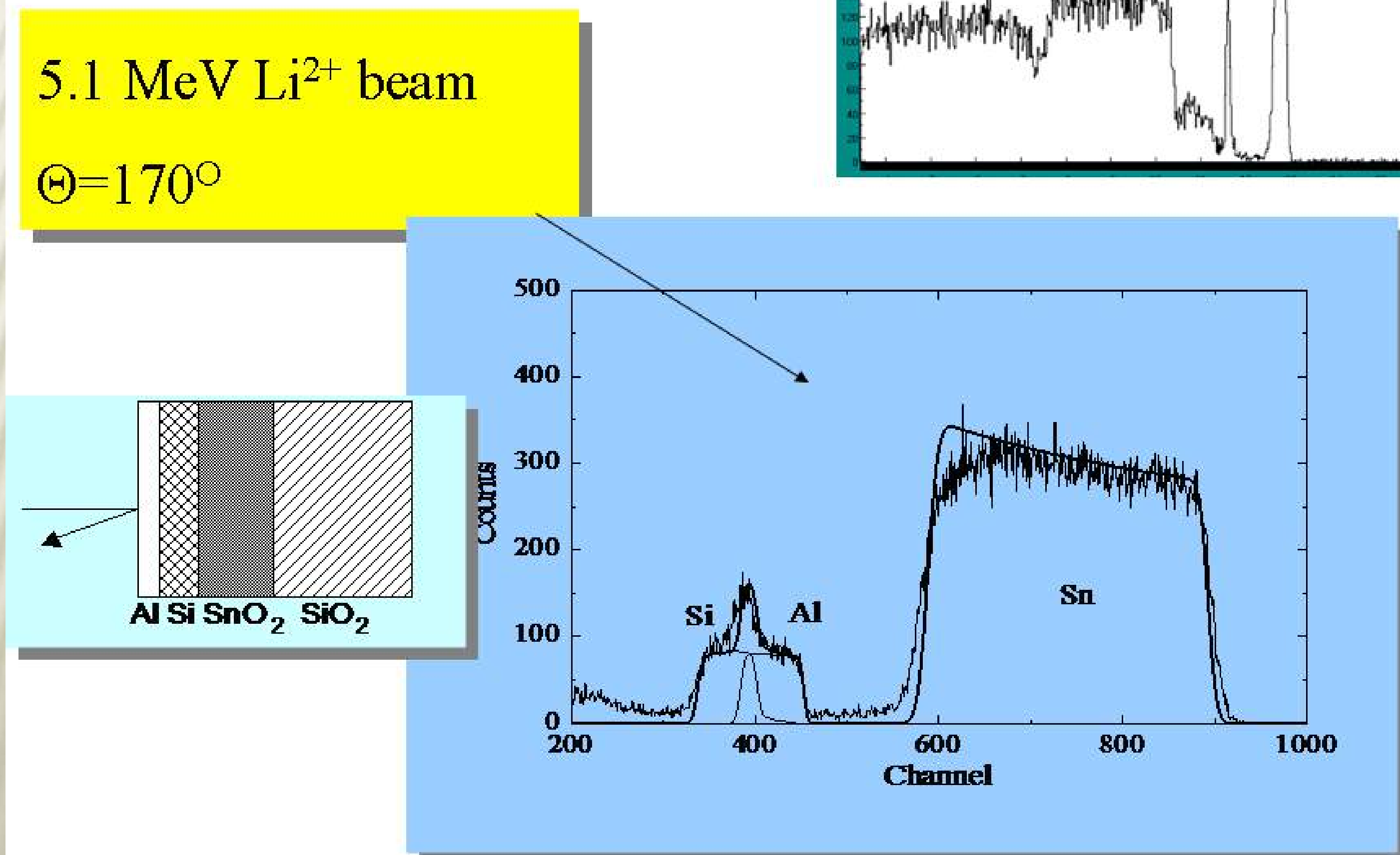

RBS –EXAMPLES

In situ RBS:
Ion beam: 2 MeV Li^7
Sample: AlCuFe thin film
Observation of layer intermixing

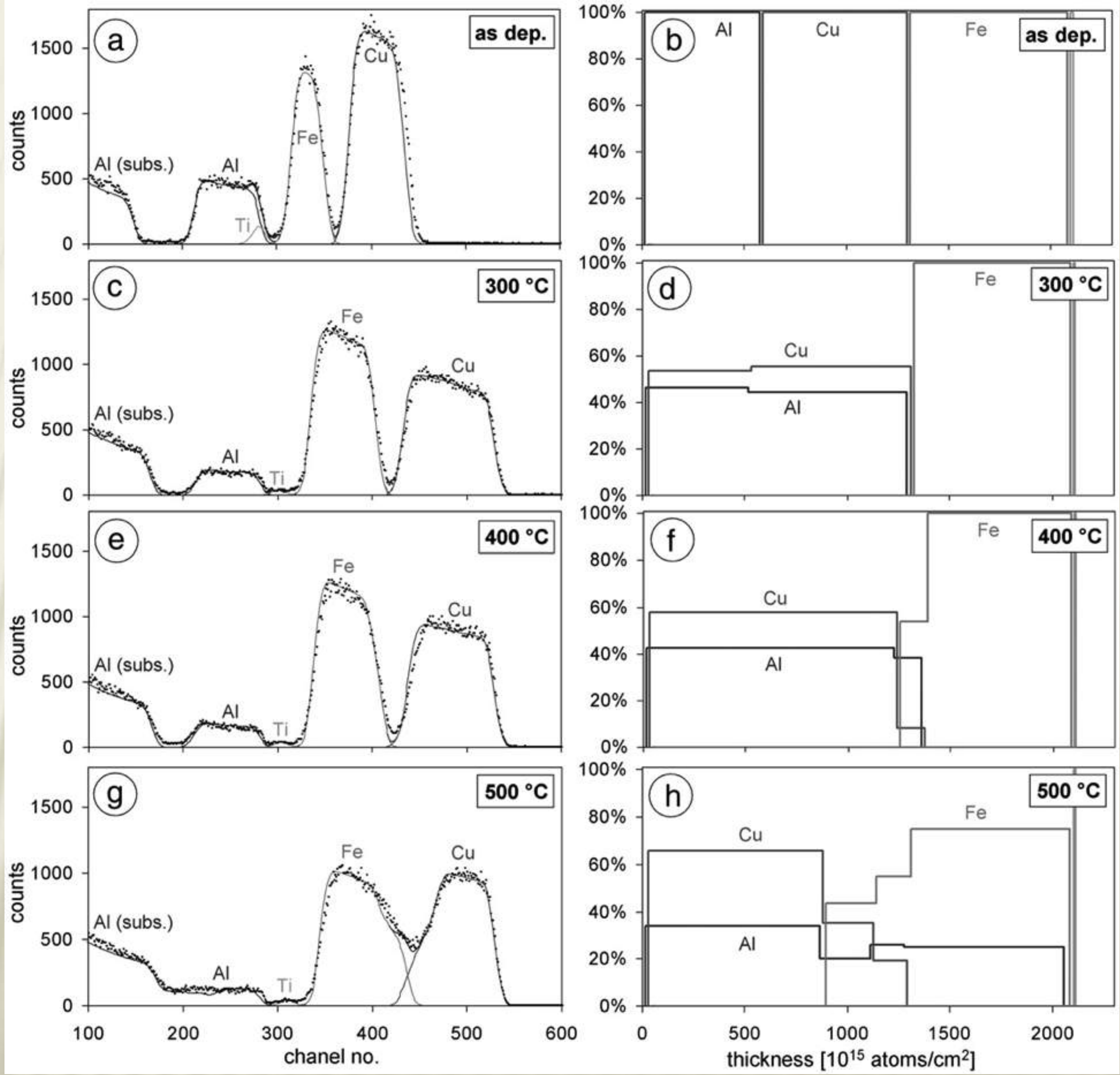

RBS –EXAMPLES

Effect of high temperature deposition on CoSi2 phase formation
C. M. Comrie, et al. J. Appl. Phys. 113 (2013)
- Identification of phase transition from CoSi to $CoSi_2$

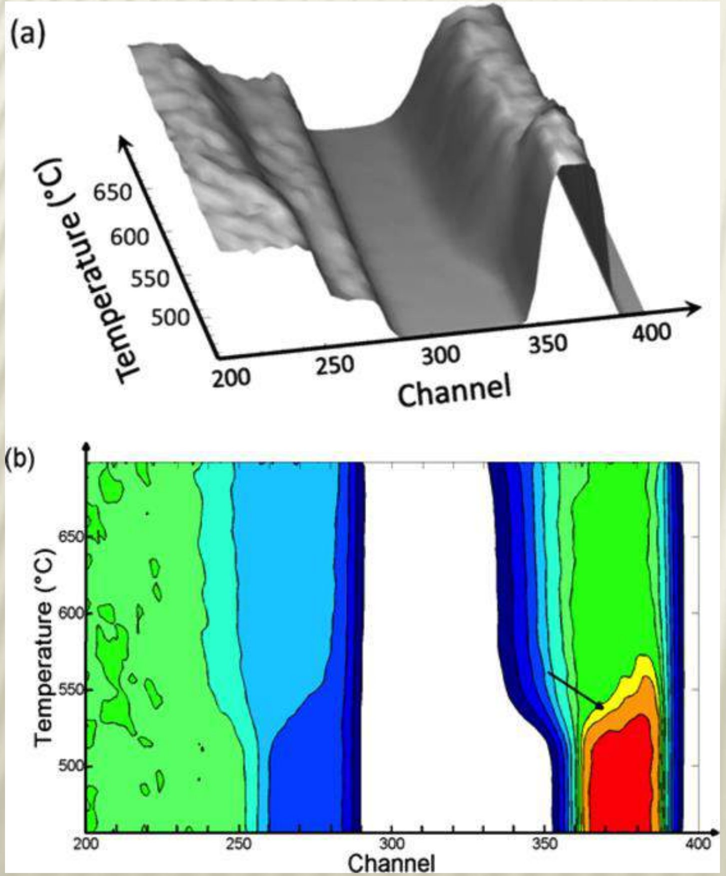

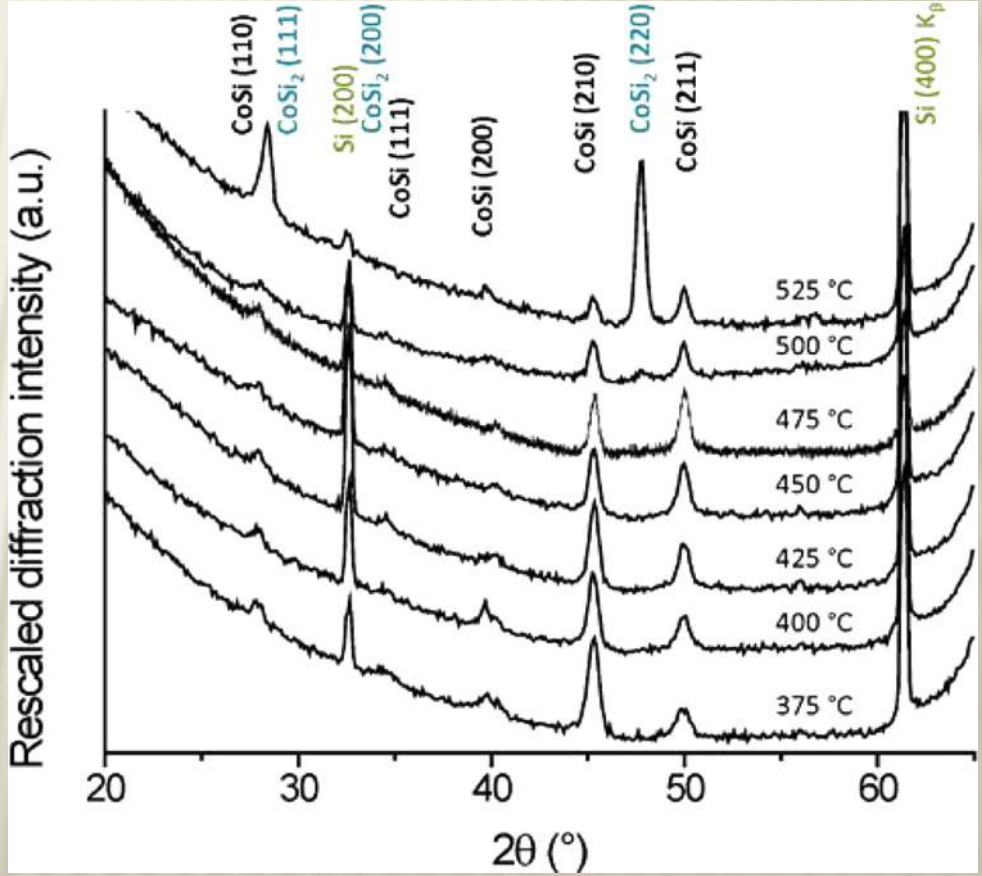

ERDA - ELASTIC RECOIL DETECTION ANALYSIS

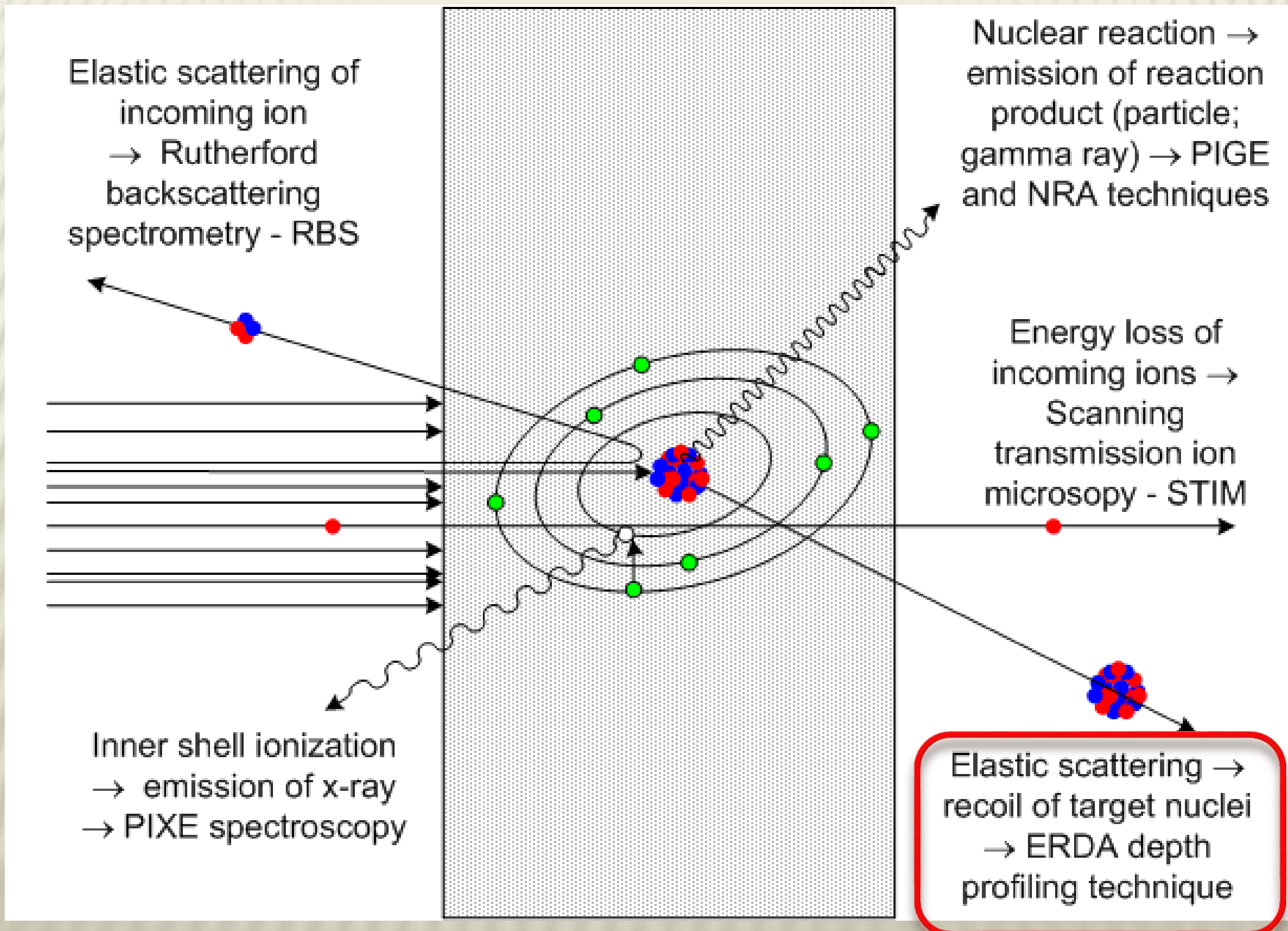

ERDA - ELASTIC RECOIL DETECTION ANALYSIS

Geometry: transmission (problems due to energy straggling) or reflection (small sampling depth)

Experimental setup:

Stopping foil – by selection of appropriate thickness, system is optimized for one particular element (e.g. Hydrogen using He ion beam)

ΔE, E detector: - scattered and recoiled particles are discriminated by different dE/dx! (energy straggling ?)

TOF, E detector:
- scattered and recoiled particles are discriminated by measurement of time of flight (with minimal straggling) – best depth resolution

+ Magnetic spectrometer (expensive)

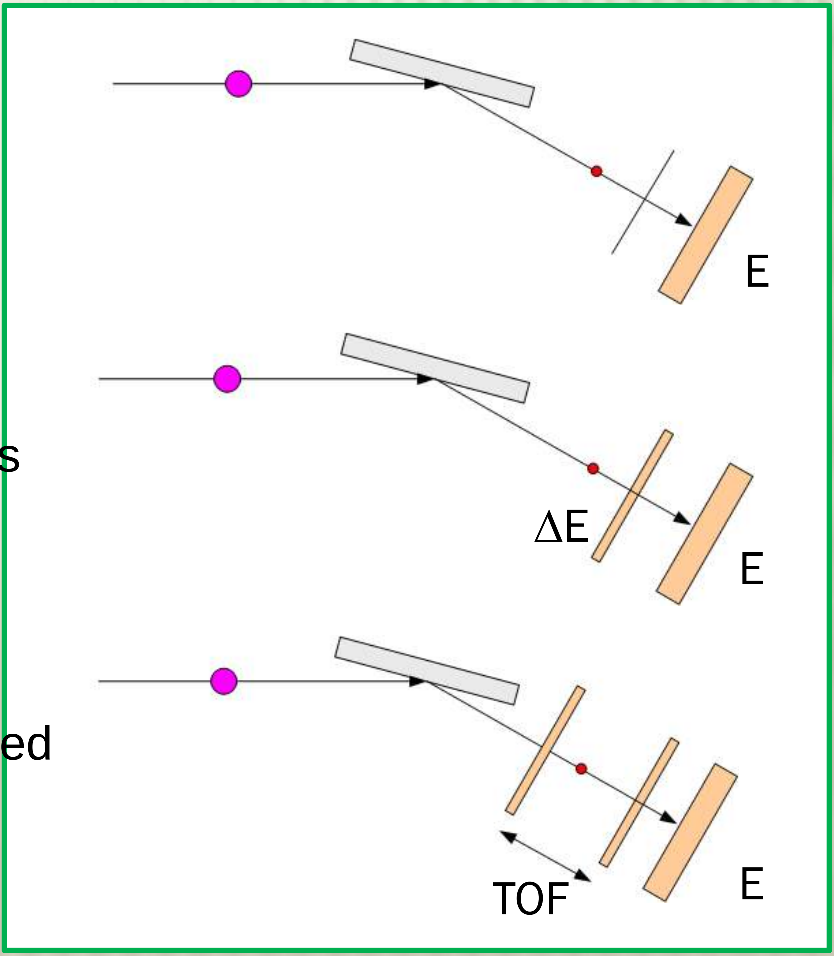

TOF - ERDA

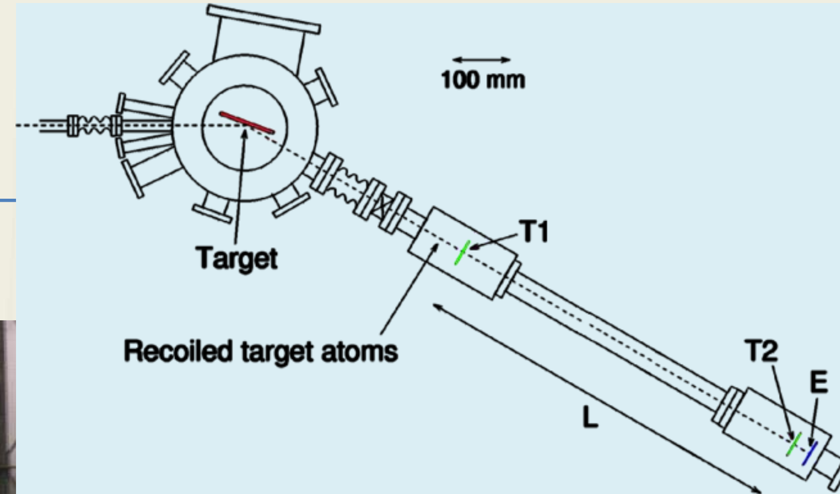
100 mm
Target
T1
Recoiled target atoms
T2
E
L

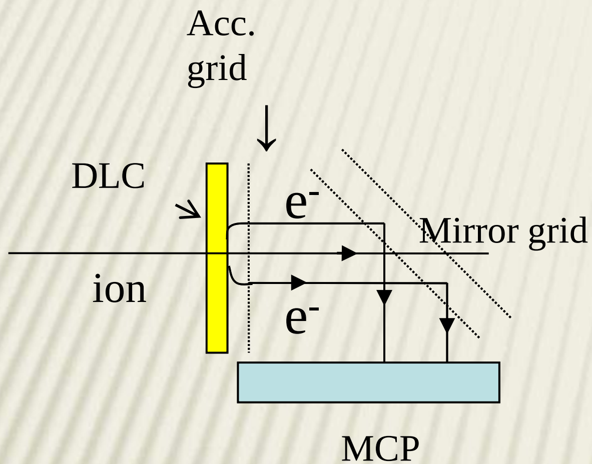
Acc. grid
DLC
e-
Mirror grid
ion
e-
MCP

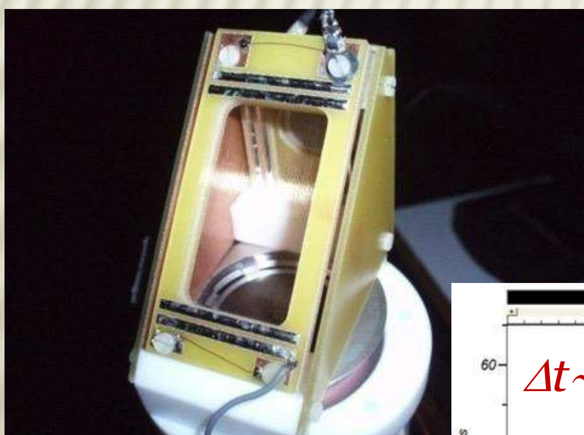

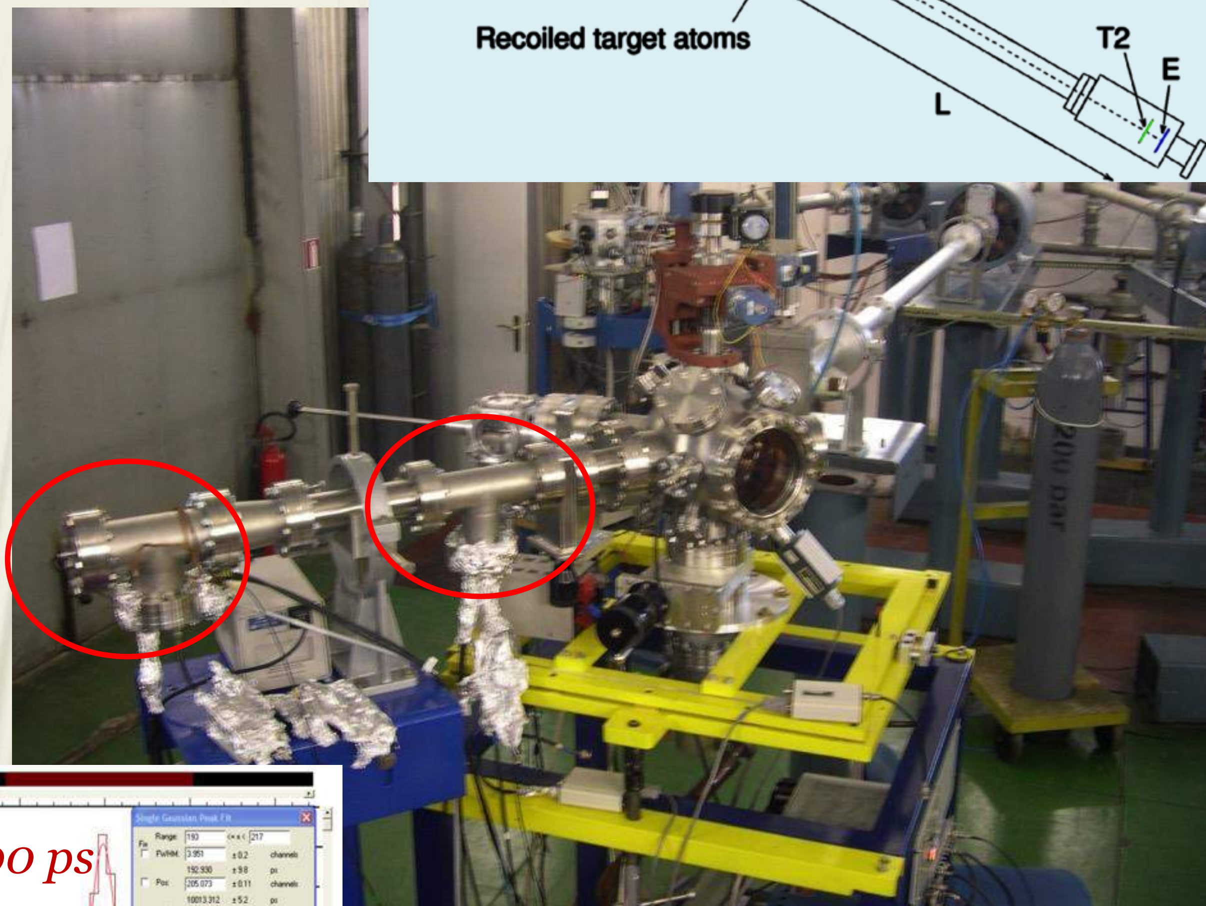

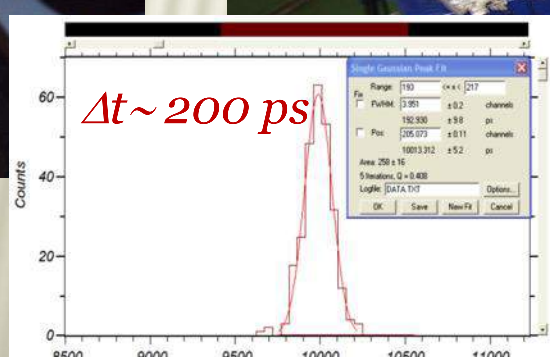
Δt~200 ps
Counts
60
40
20
0

TOF - ERDA

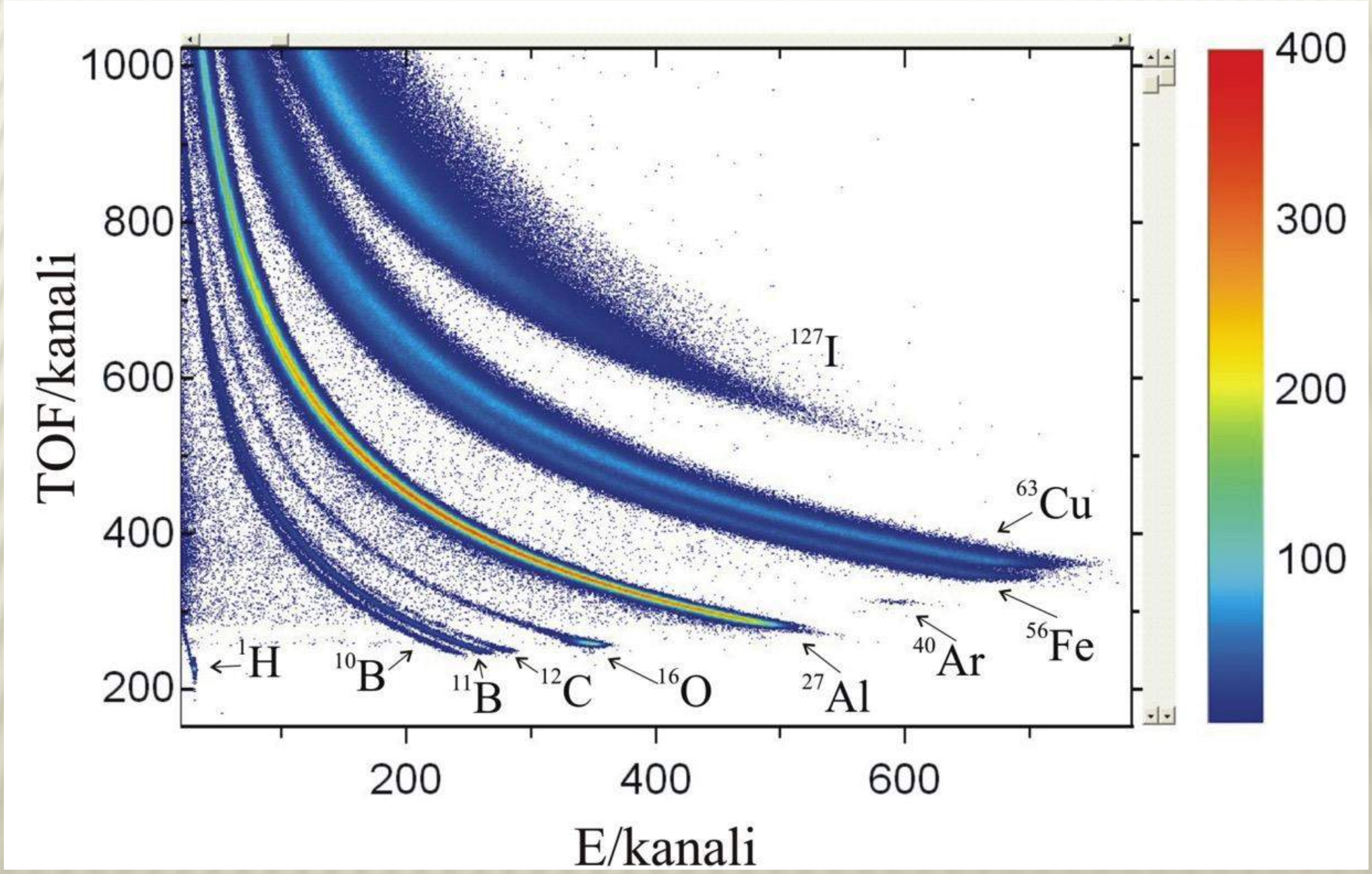

TOF/kanali
1000
800
600
400
200
E/kanali
200
400
600
400
300
200
100
127I
63Cu
56Fe
40Ar
27Al
16O
12C
11B
10B
1H

TOF - ERDA

Heavy ion beam – e.g. 20 MeV Iodine ions

- sensitivity 10^{15} /cm^2
- 5 nm depth resolution, up to 500 nm probe depth
- all elements are resolved

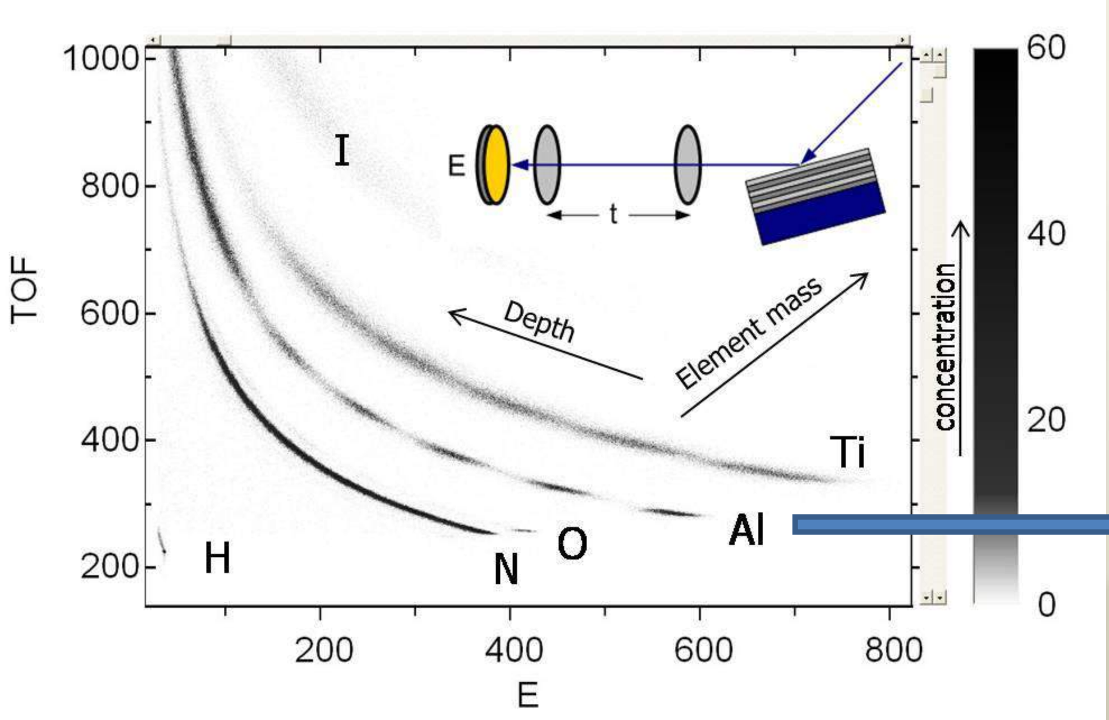

Sample:
20 nm multilayers TiN/AlN

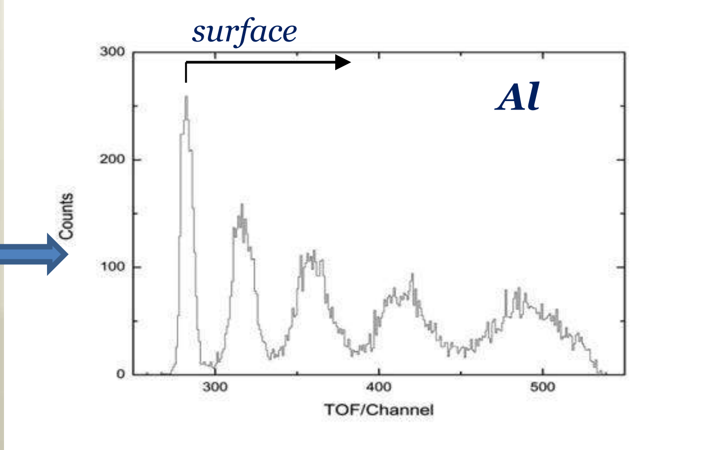

TOF - ERDA

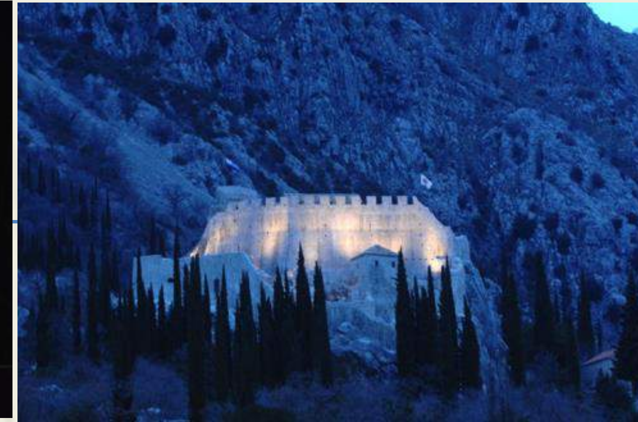

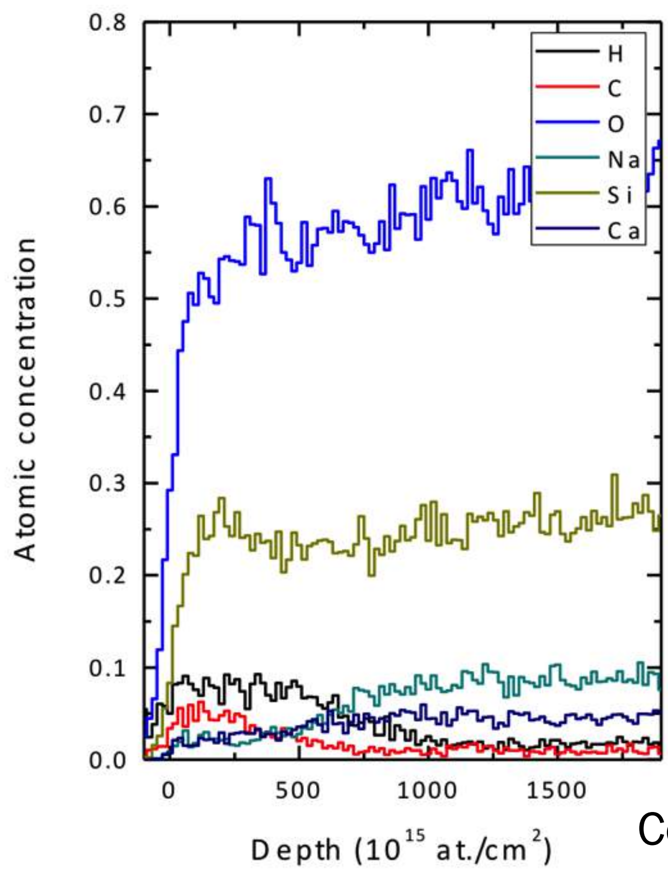

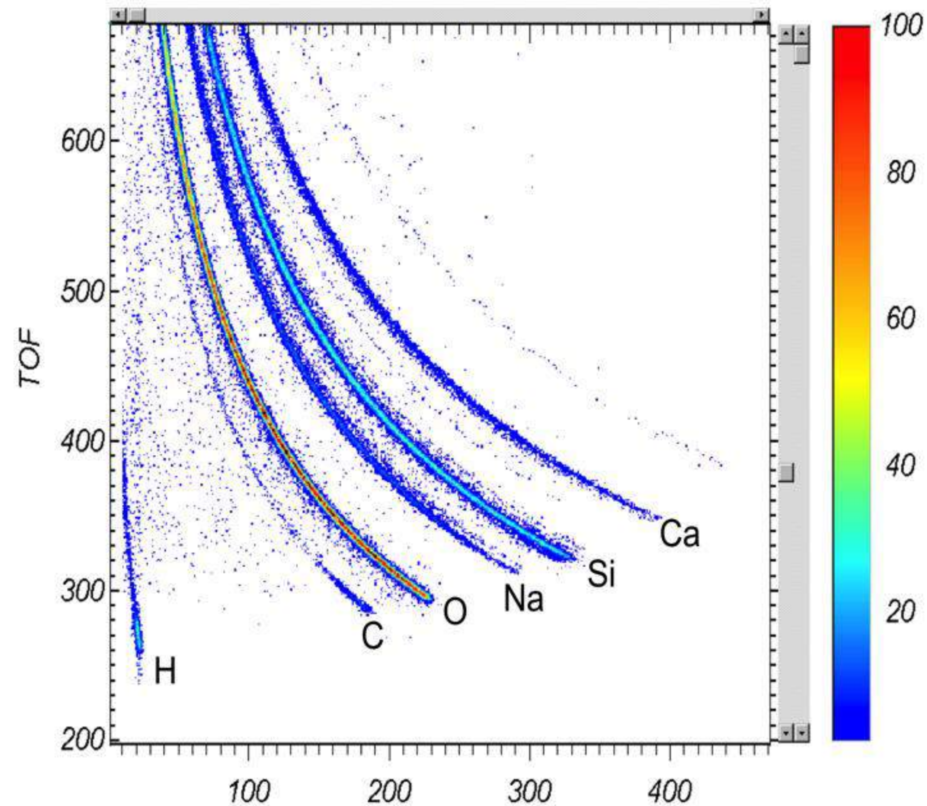

Corrosion of ancient glass found at the fort Sokol (close to Dubrovnik airport)

PARTICLE INDUCED X-RAY EMISSION SPECTROSCOPY

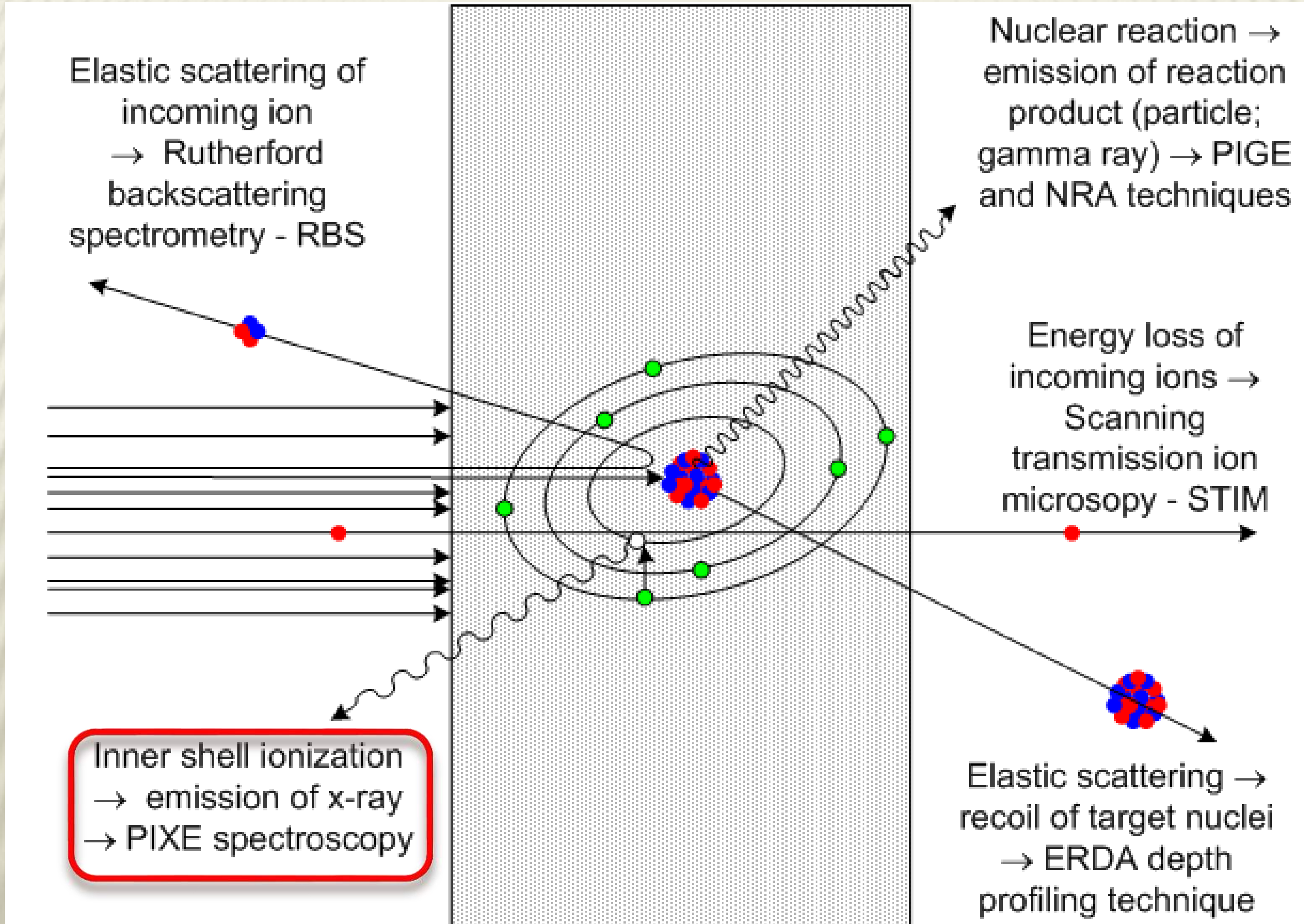

PIXE

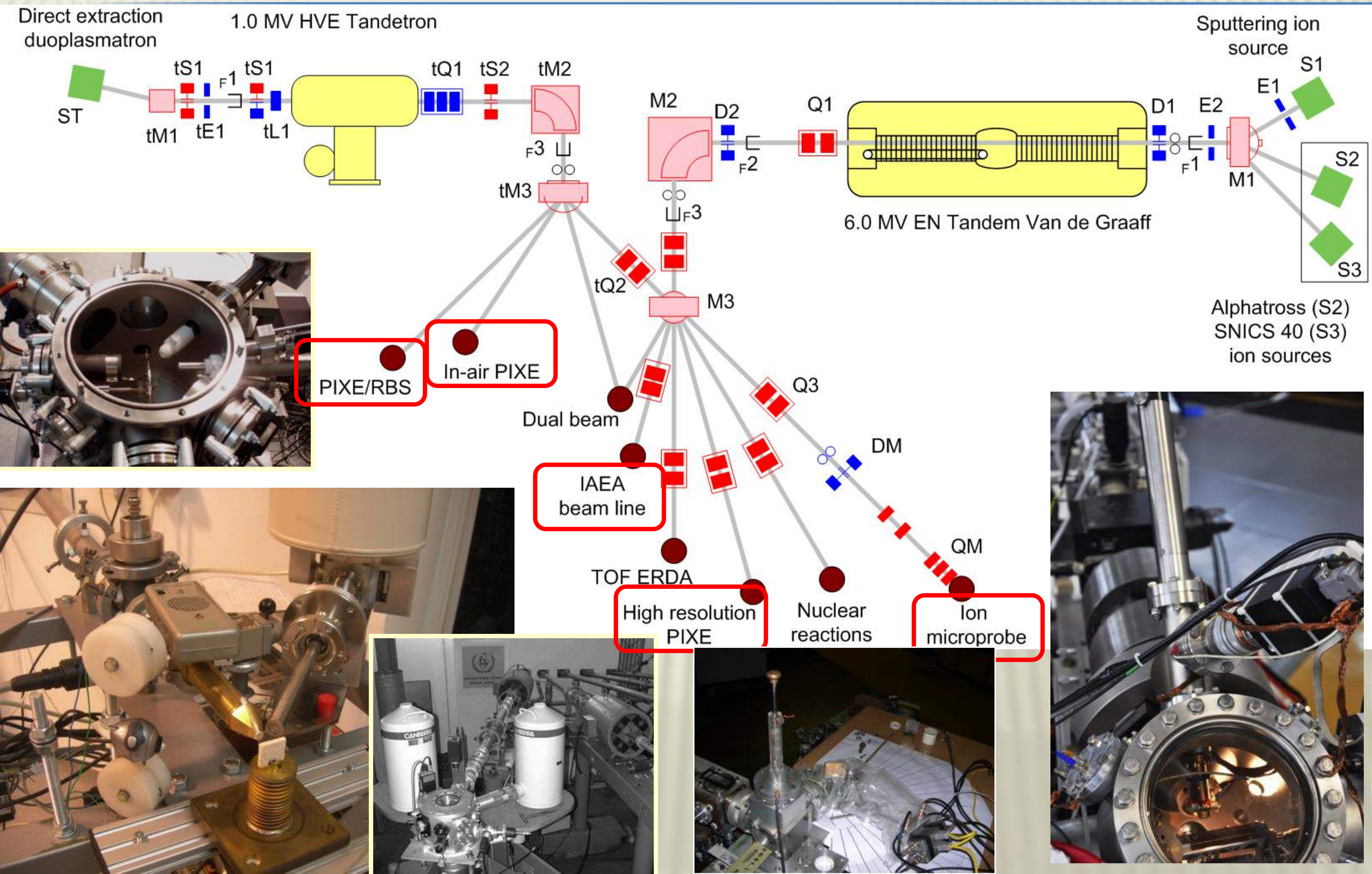

Direct extraction duoplasmatron
1.0 MV HVE Tandetron
Sputtering ion source
ST
tS1
F1
tS1
tM1
tE1
tL1
tQ1
tS2
tM2
F3
tM3
M2
D2
F2
Q1
D1
E2
F1
E1
S1
M1
S2
S3
F3
6.0 MV EN Tandem Van de Graaff
tQ2
M3
Alphatross (S2)
SNICS 40 (S3)
ion sources
PIXE/RBS
In-air PIXE
Dual beam
Q3
DM
IAEA beam line
TOF ERDA
QM
High resolution PIXE
Nuclear reactions
Ion microprobe

PIXE

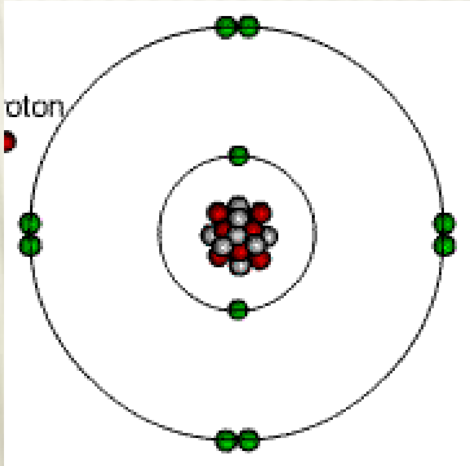

Simple quantification for thin targets:

$Y_i = Q/e\ C_i\ \Omega\varepsilon\ \sigma_i$

Q/e – fluence

$\Omega\varepsilon$ – detector solid angle and efficiency

σ_i – production cross section

$\sigma_i = \sigma_{ii}\ \omega$, where σ_{ii} is ionization cross section and ω fluorescence yield

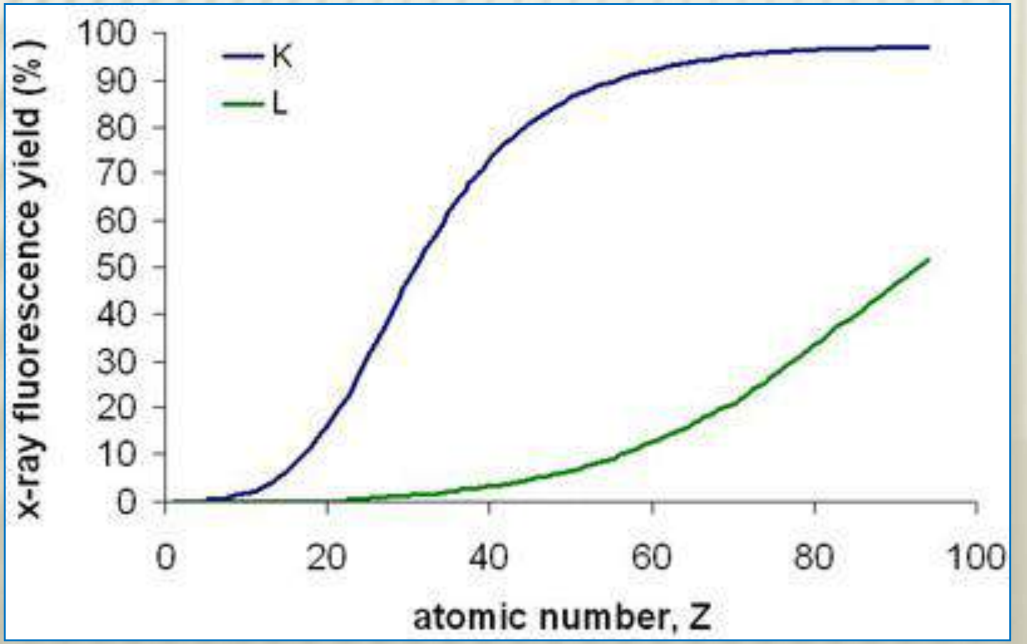

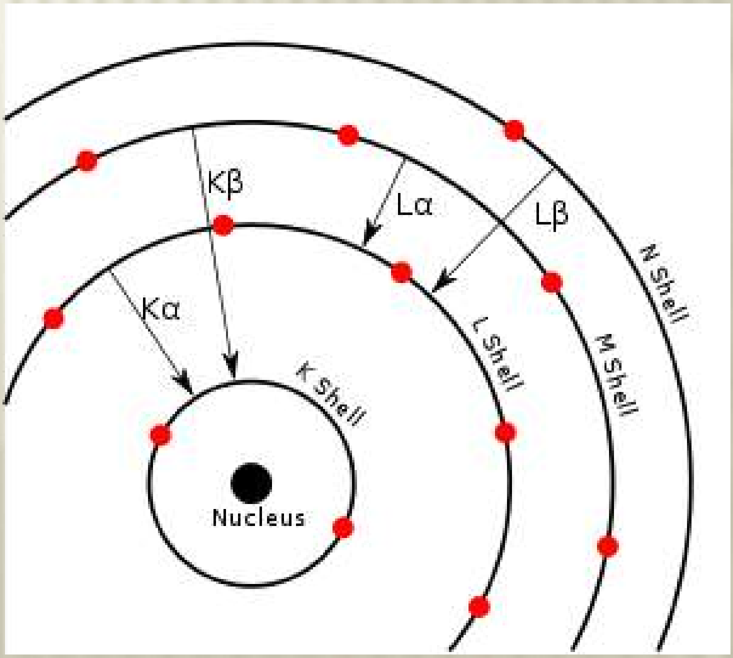

PIXE

For thick targets, quantification is becoming more complicated !!

$$Y_i = \frac{Q}{e}\int_0^d c(x)\sigma_i(E(x))e^{-\mu x/\sin\vartheta}dx$$

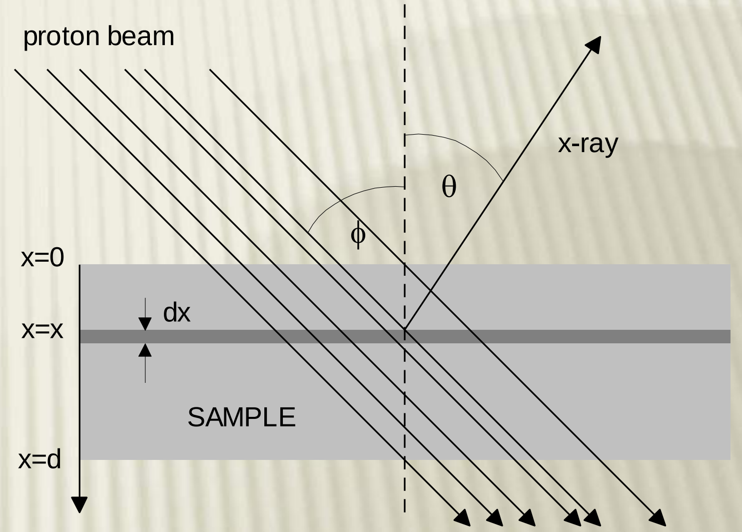

Yield depends on composition due to Ion stopping & x-ray absorption:

a) Iterative procedure, or
b) Matrix composition from other techniques (RBS) !!

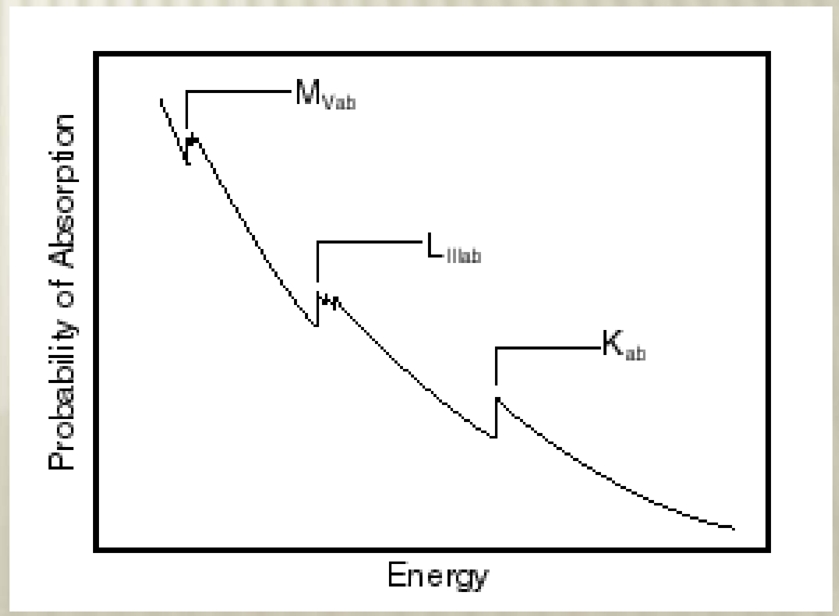

PIXE ANALYSIS

air polution monitoring

Nucleopore Track-Etched Membrane

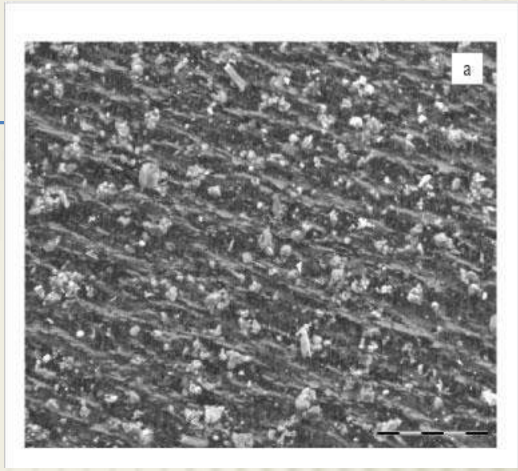

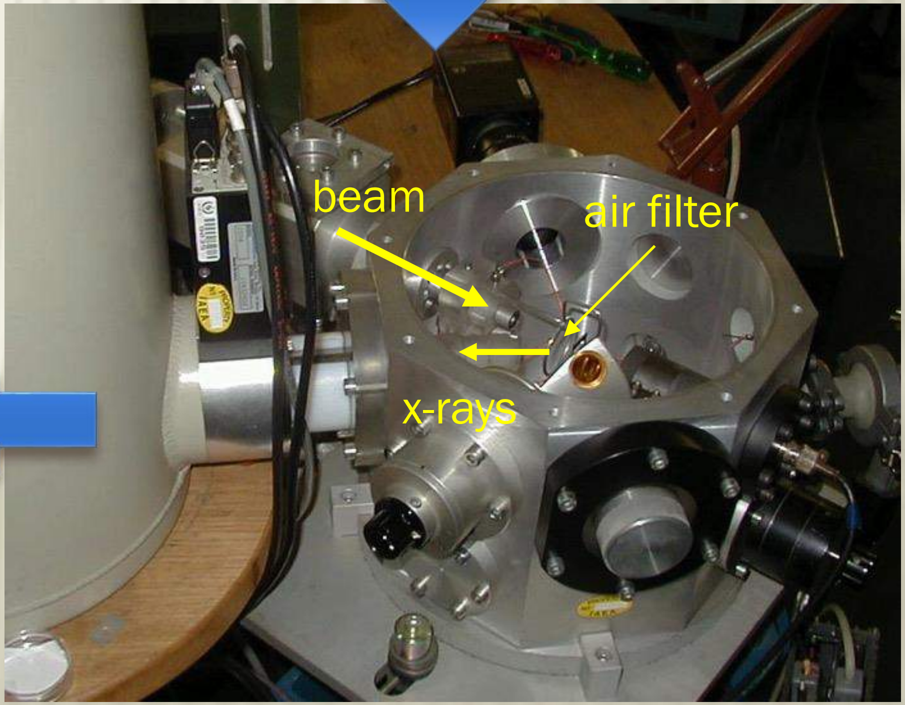

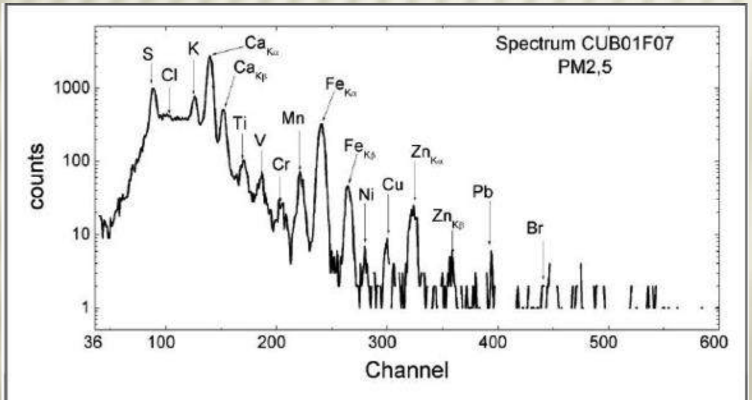

Figure 2. Representative PIXE spectra of the fine airborne particulate matter collected in the sampling site.

PIXE ANALYSIS

air polution monitoring

	MDL	No01	No02	No03	No04	No05	No06	No07	No08	No09	No10	No11	No12	No13	No14	No15
Ca	5.3			29.2	33.2	62.9	17.5	34.9	75.0		27.2	115.8			24.1	35.1
Ti	2.8	4.0		3.6								5.0	4.8	4.0		
V	2.0	2.0		2.6	2.9	4.3		3.9	3.2	2.9	4.3	8.2	15.7	5.3	2.6	
Cr	1.5					2.2						2.0	2.7		1.7	
Mn	1.3	6.2	7.3	7.0	6.8	11.0	6.7	9.1	2.7	6.0	7.9	28.0	17.2	8.7	7.0	4.5
Fe	0.9	72.5	119.6	113.2	93.8	154.9	90.7	140.8	50.9	102.3	152.9	239.2	196.1	98.5	105.8	86.2
Ni	0.8	2.0		2.4	1.7	2.5	0.9	2.5	2.0	1.8	2.6	4.8	8.4	3.7	1.0	1.1
Cu	0.6	22.2	10.7	6.4	6.4	10.5	5.1	8.0	2.9	6.1	15.5	20.5	20.3	12.6	7.1	5.4
Zn	0.8	28.9	18.1	15.7	19.5	64.5	25.9	34.9	13.0	22.7	36.9	62.1	121.2	75.7	25.2	19.8
As	1.6										1.8	2.3	2.4			
Br	0.8	5.7	4.8	5.9	0.8	1.3		1.7				1.1	0.9			1.4
Rb	0.9					1.1						2.2	2.7	2.6	1.2	
Sr	1.1	10.2														
Zr	1.3															
Mo	2.1															
Ba	11.2															
Pb	2.7	29.4	20.0	15.4	12.7	60.5	14.0	19.5	7.4	25.2	36.6	49.4	129.8	55.1	16.9	10.5

	No16	No17	No18	No19	No20	No21	No22	No23	No24	No25	No26	No27	No28	No29	No30	No31
Ca	31.9	99.9	49.0		55.0	78.8	98.6	42.4	31.8	59.5	95.7	59.5	23.6	12.6	98.2	15.9
Ti		3.5				3.4					2.9					2.9
V		8.8	5.9	5.6	5.7	4.3						3.0				6.0
Cr					1.6											
Mn	4.2	7.9	5.3	8.2	5.5	11.6	5.2	3.5	1.7	1.7	2.5	3.2	3.9	4.1	5.2	5.7
Fe	85.5	129.2	69.7	120.5	81.1	184.3	80.4	56.8	17.9	32.1	31.8	42.2	44.7	42.0	60.1	82.6
Ni		3.8	4.0	3.8	2.5	1.1		0.9						1.1	2.6	2.9
Cu	5.3	12.1	5.3	7.7	6.3	9.2	4.8	3.2	0.9	1.9	2.0	3.5	2.6	4.9	9.7	5.0
Zn	18.4	53.9	45.4	35.7	31.0	36.1	17.4	14.3	10.6	23.5	30.2	28.7	37.9	30.6	39.7	24.5
As		1.9	1.7											1.7	0.0	
Br	1.1	5.2	2.5	3.0	2.4	4.4	1.2	1.0	1.0	1.7	0.9	2.3	1.9	0.8	3.0	5.0
Rb			1.3		1.3	1.2						0.8		1.3	1.1	1.0
Sr																
Zr																
Mo																
Ba																
Pb	11.1	27.6	48.8	28.3	18.4	20.9	8.2	10.6	4.2	10.6	9.9	11.9	13.6	10.7	21.3	12.8

PIXE ANALYSIS

air polution monitoring

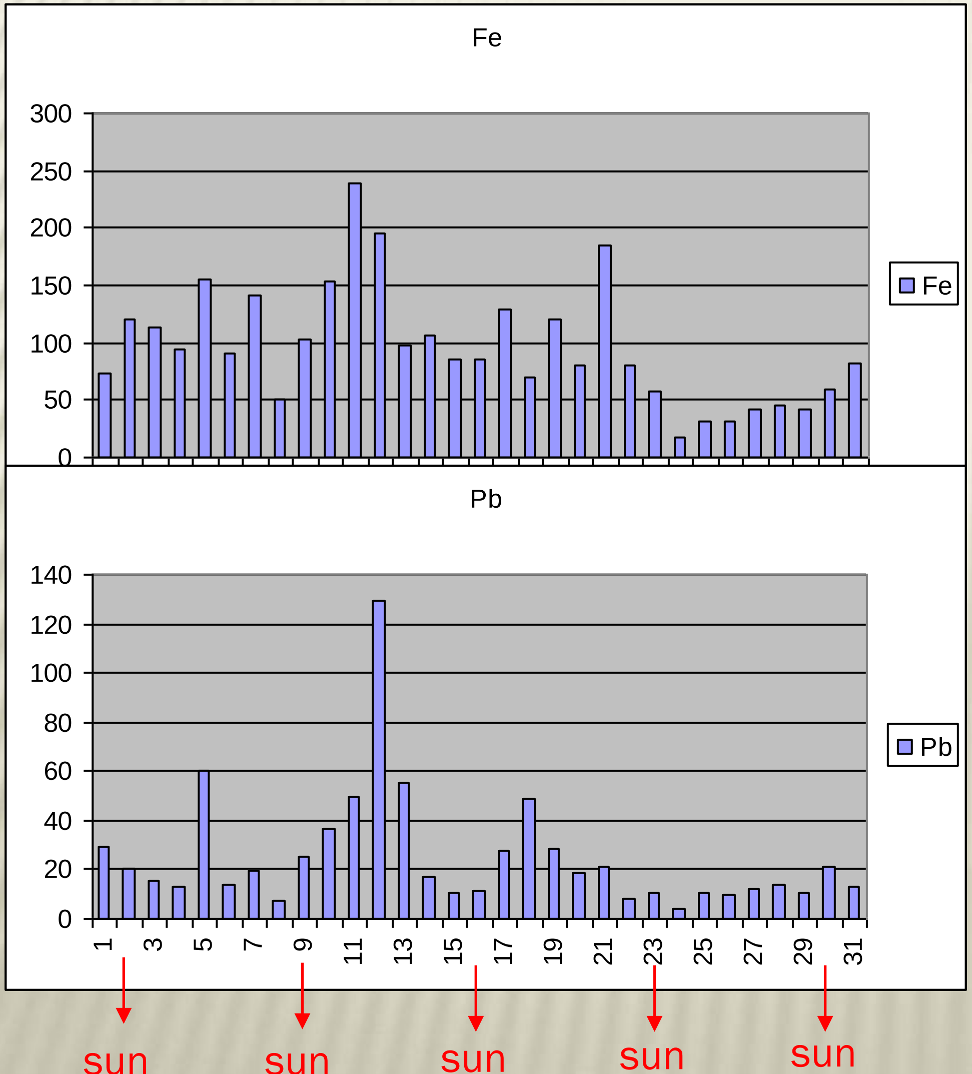

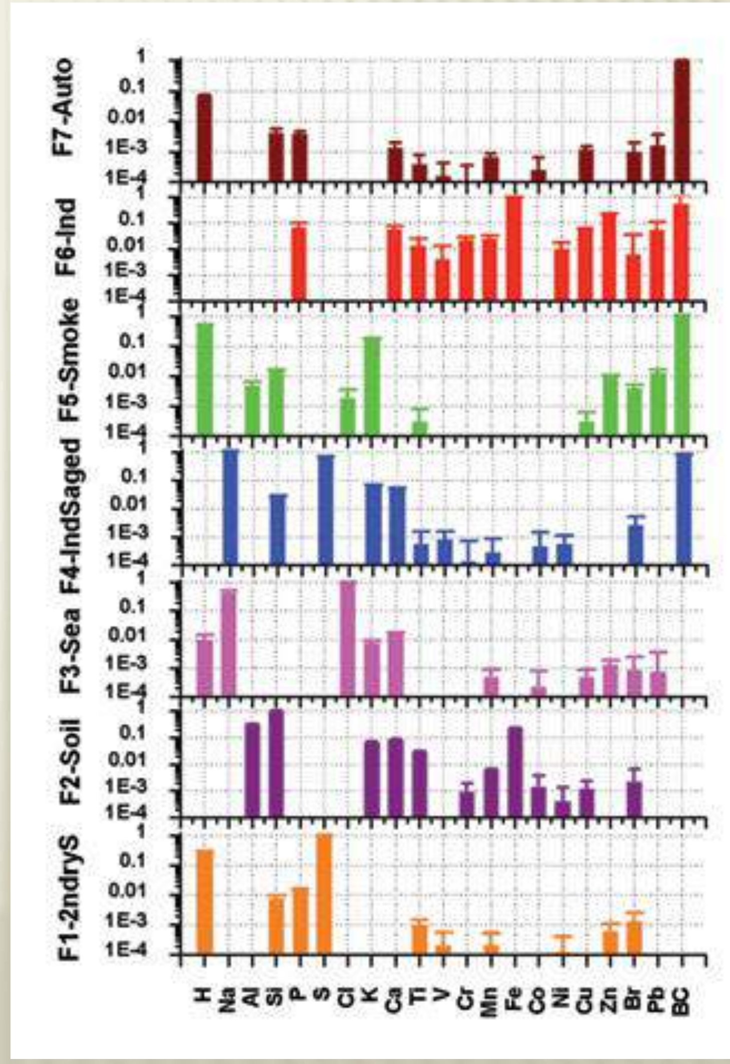

In air PIXE ANALYSIS

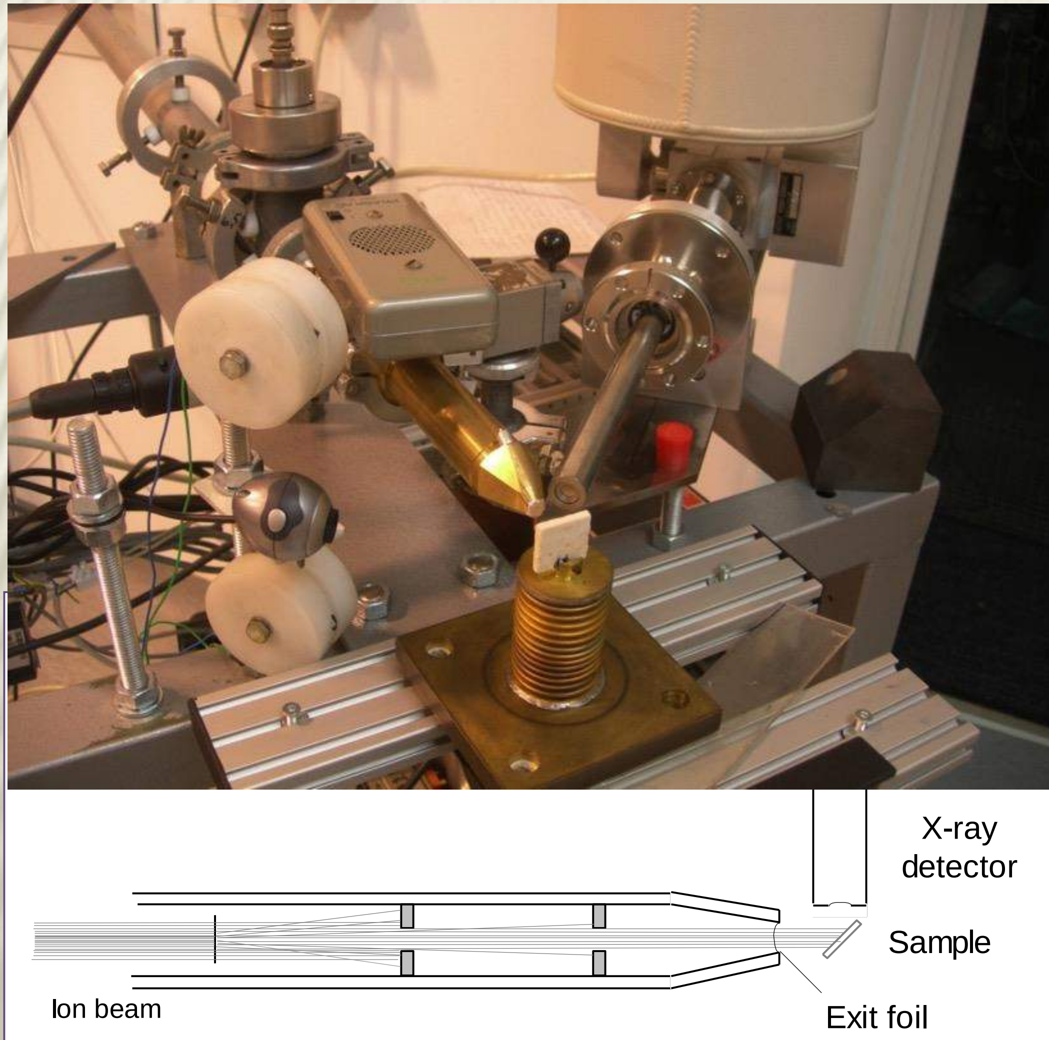

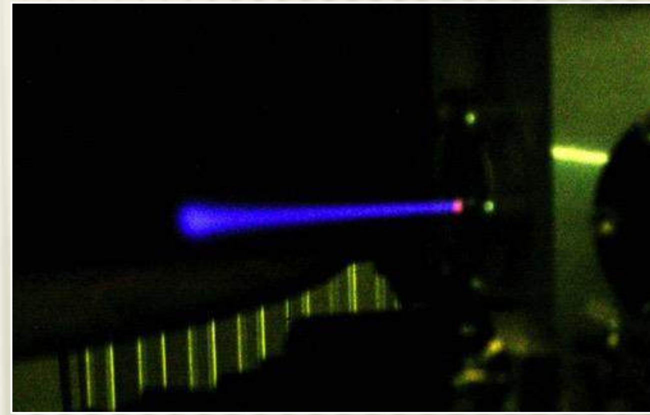

ion/energy	range in air (mm)
p, 1 MeV	23.25
p, 2 MeV	71.25
p, 3 MeV	**140.52**
α, 1 MeV	5.21
α, 2 MeV	10.24
^{12}C, 3 MeV	5.21
^{28}Si, 6 MeV	6.27

PIXE APPLICATIONS – CULTURAL HERITAGE

Analysis of helmet

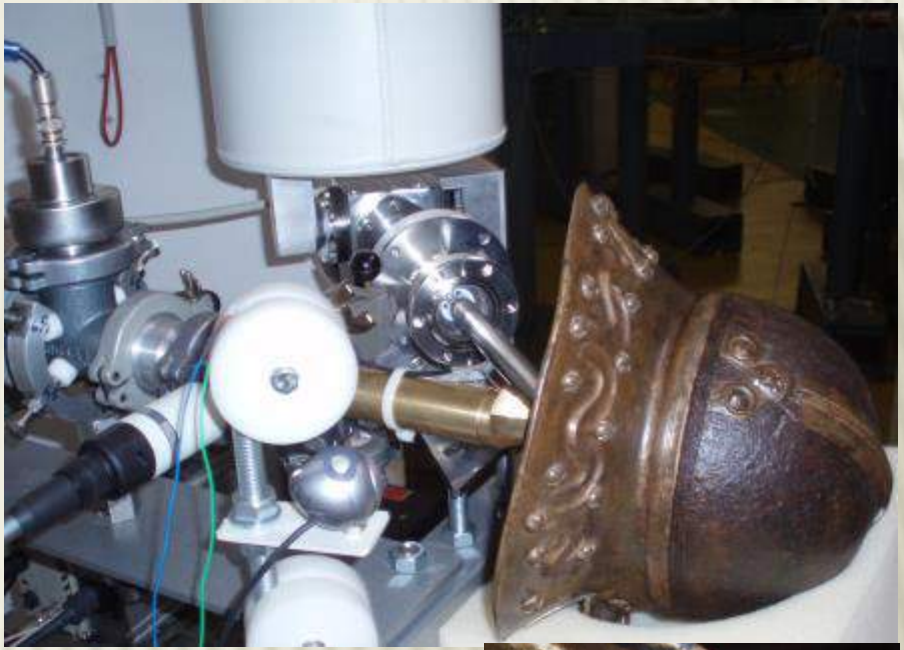

file uzorak

705231 Kaptol-G. T-6 kaciga
705232 Kaptol-G. T-6 PN80 drška mača (crvenkasta površina)
705233 isto (zelenkasta površina)
705234 Kaptol-G. T-6 korice mača
705235 štrb.13.06.05. PN3, SJ1/2, B48, vjerG.104, pixe, A, 1,20g
705236 4029-Sl.Brod, SEOM KNEMIDA

Spektar	Si	P	S	Cl	K	Ca	Fe	Cu	Sn	Pb
705231	1		0.4	0.2			0.9	**73.8**	**17**	3.2
705232	1.6			1			2.1	**57.6**		**34.4**
705233	**6.2**	0.5	0.5	0.3	0.3	0.5	**5.6**	**71.2**	0.9	**10.3**
705234	1.9		0.3	0.4			0.1	**78.0**	**15.0**	1.5
705235	**5.3**	**9.0**	2.7			**5.2**	1.4	**6.4**	**29.0**	**32.8**
702356	1.4	1.6	0.2	0.8			0.3	**66.5**	**25.0**	1.6

PIXE APPLICATIONS – CULTURAL HERITAGE

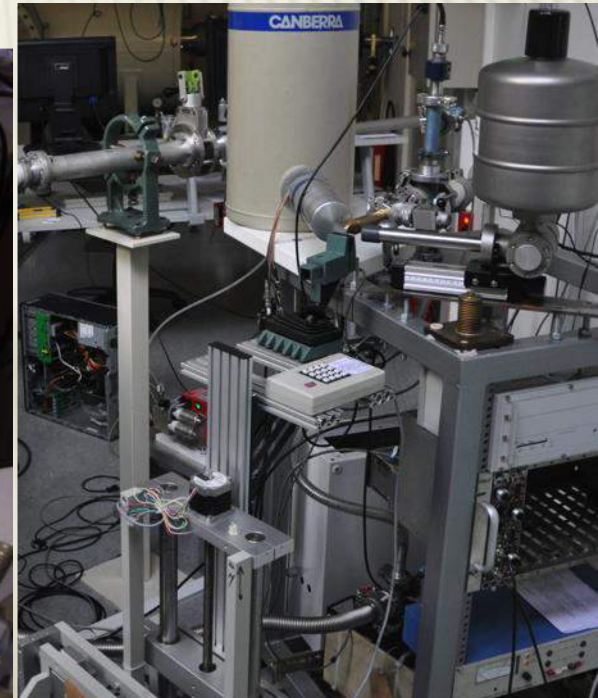

X-ray detector

Ion beam
(1 mm diameter)

Simple external beam setup:
- Robust Al foil exit window
- No additional vacuum pump required
- Classical Si(Li) detector
- Computer controlled XYZ table

PIXE APPLICATIONS – CULTURAL HERITAGE

Analysis of technology used to make Roman silver plate
(found recentely in town Vinkovci, Croatia)

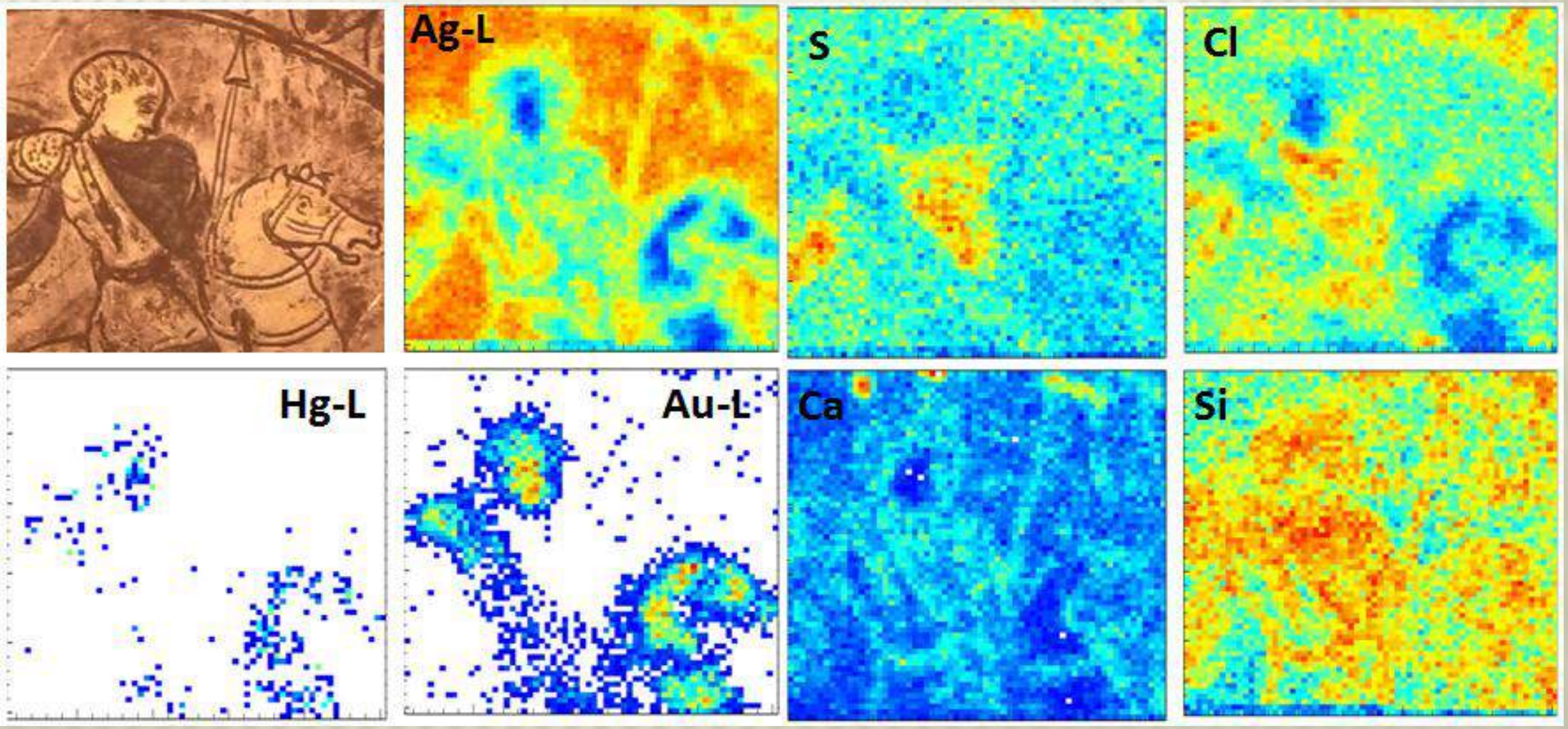

Proton beam collimated to ϕ < 1 mm; Scanned area 3 x 3 cm

NUCLEAR MICROPROBE

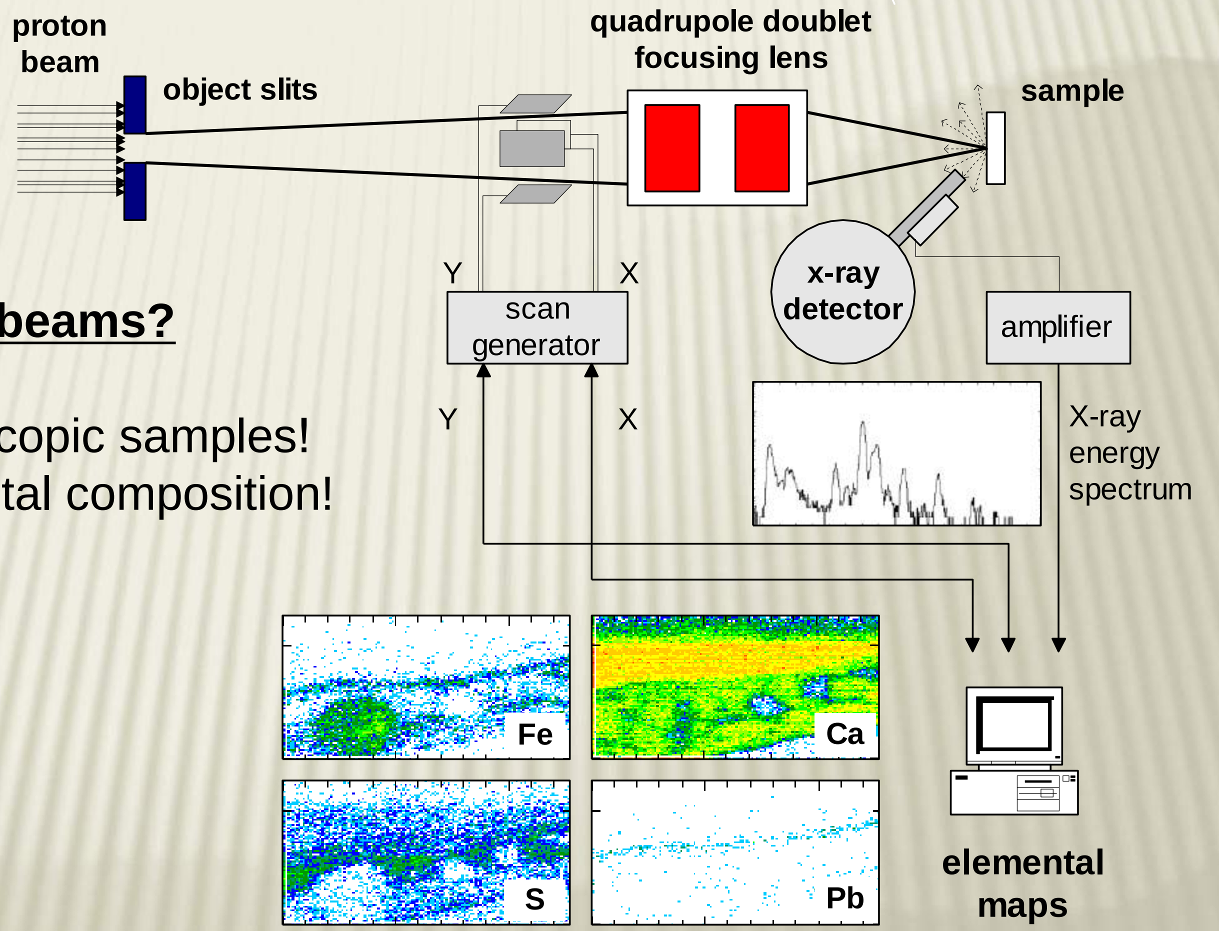

<u>Why we need microbeams?</u>

- Analysis of microscopic samples!
- Imaging of elemental composition!

NUCLEAR MICROPROBE

Available configurations at RBI:

Doublet (Dx = 11 Dy = 67)

Triplet (Dx = 30 Dy = 102)

Quintuplet (Dx=90 Dy=110)

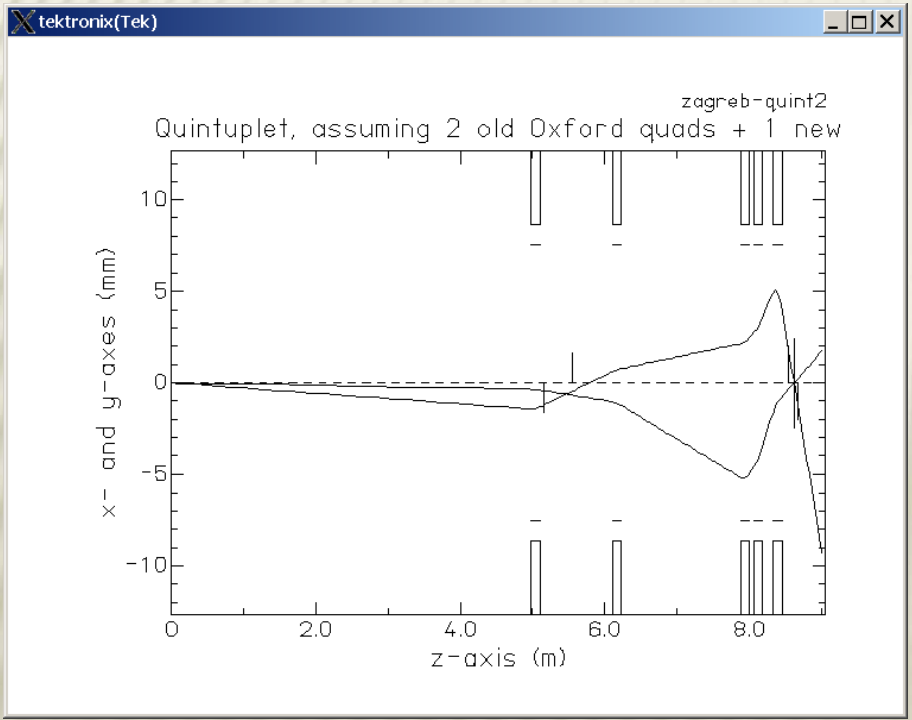

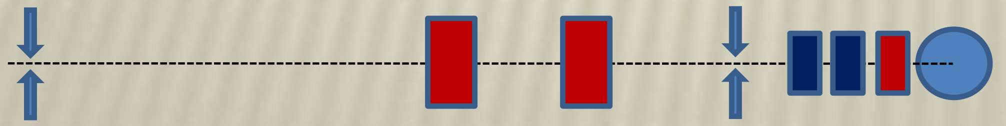

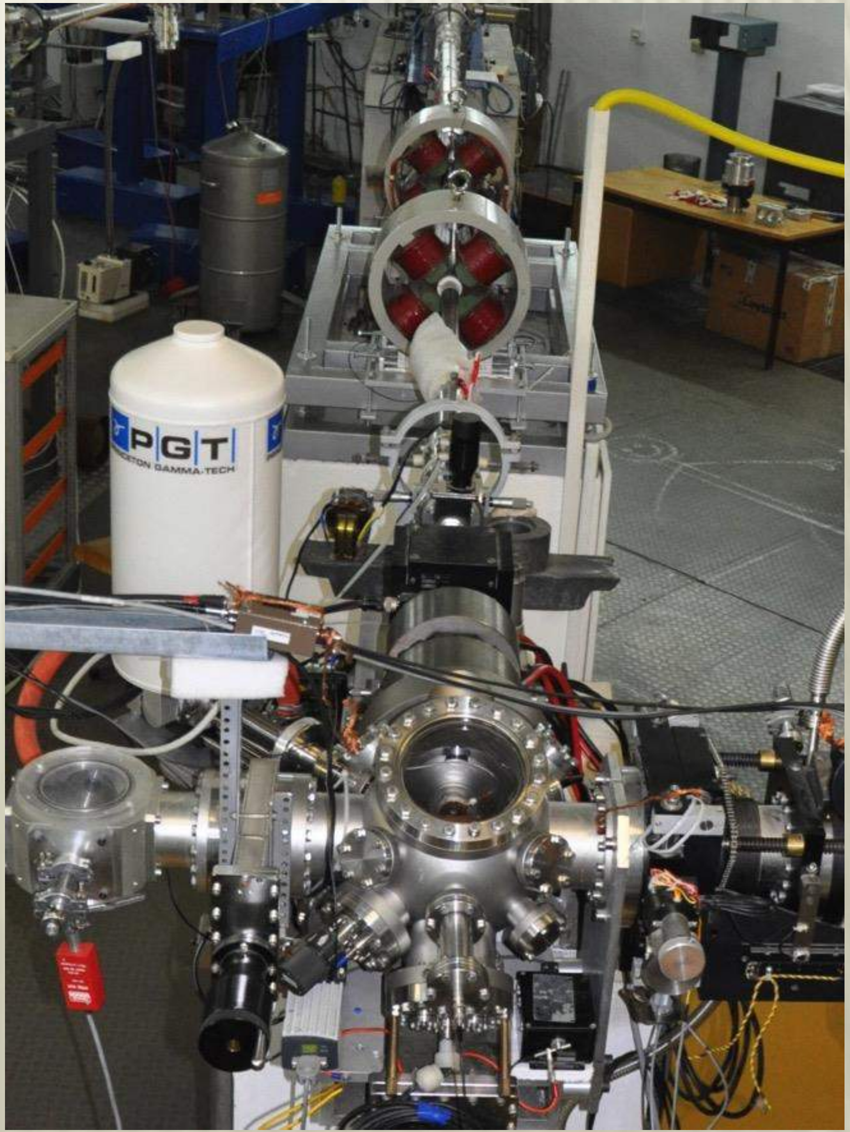

NUCLEAR MICROPROBE

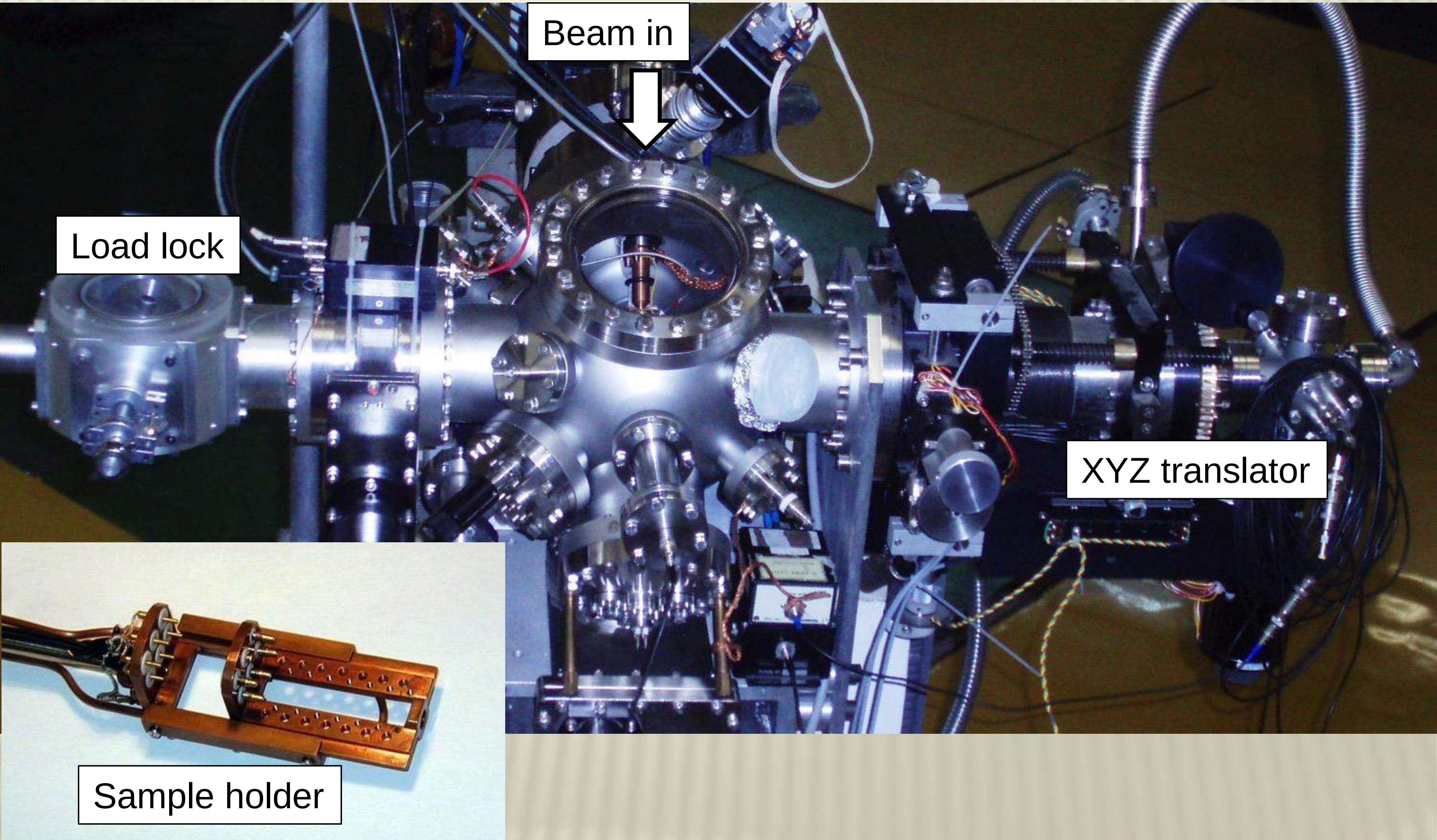

NUCLEAR MICROPROBE

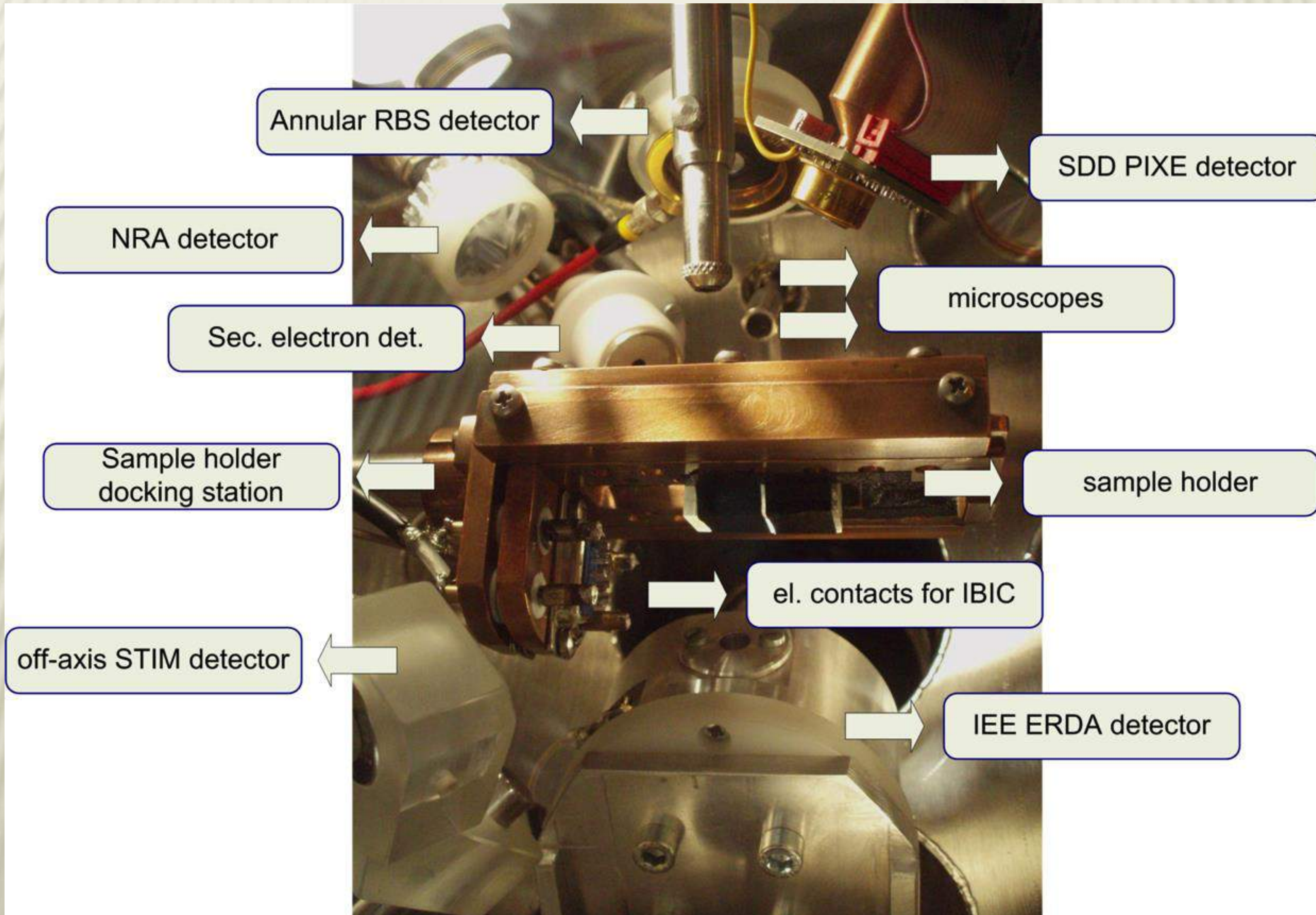

NUCLEAR MICROPROBE – PIXE APPLICATIONS

environment

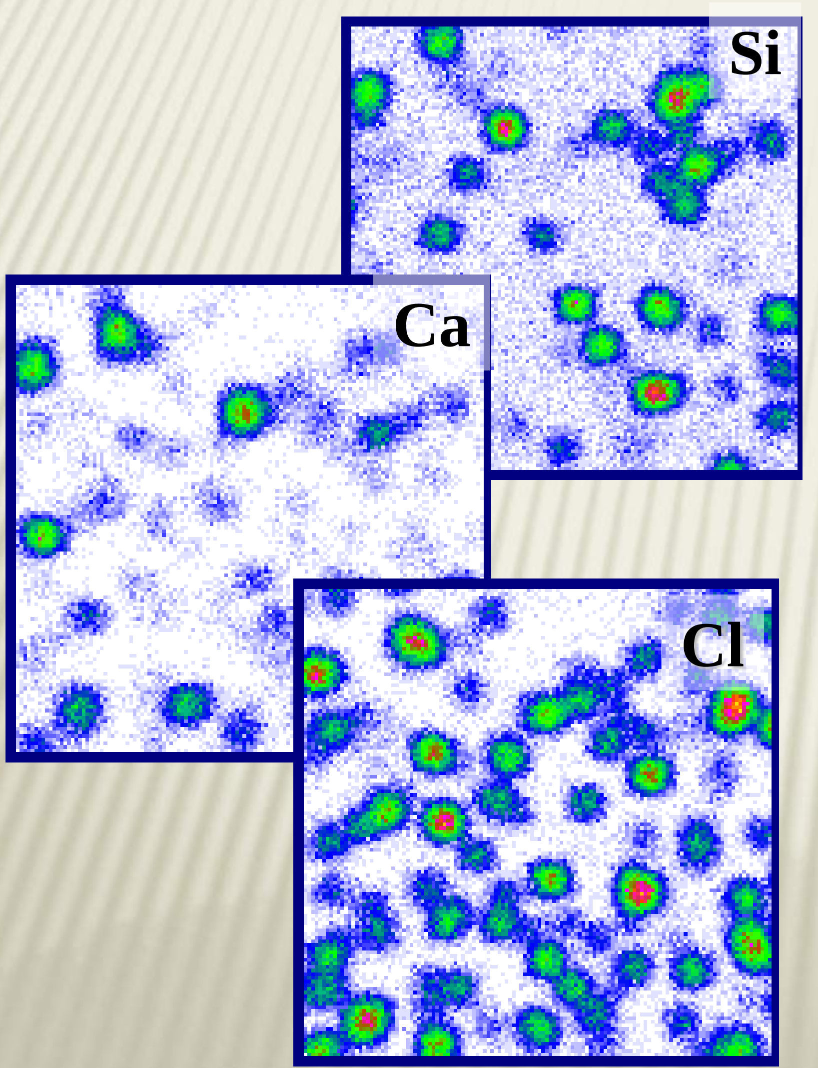

Analysis of single airparticulates for identification of sources of pollution: Na, Cl – sea salt

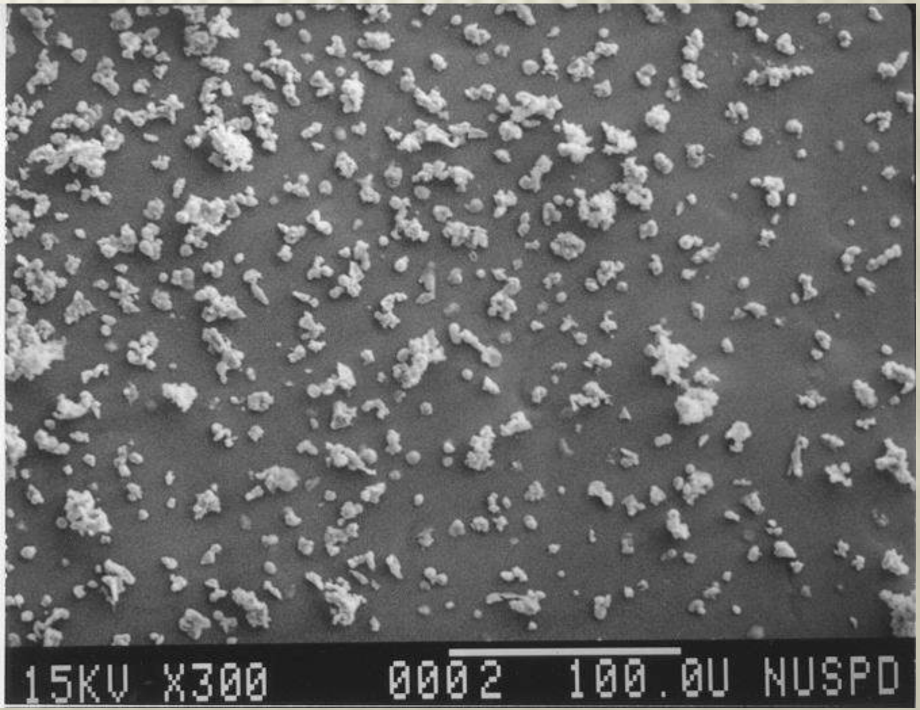

NUCLEAR MICROPROBE – PIXE APPLICATIONS

environment

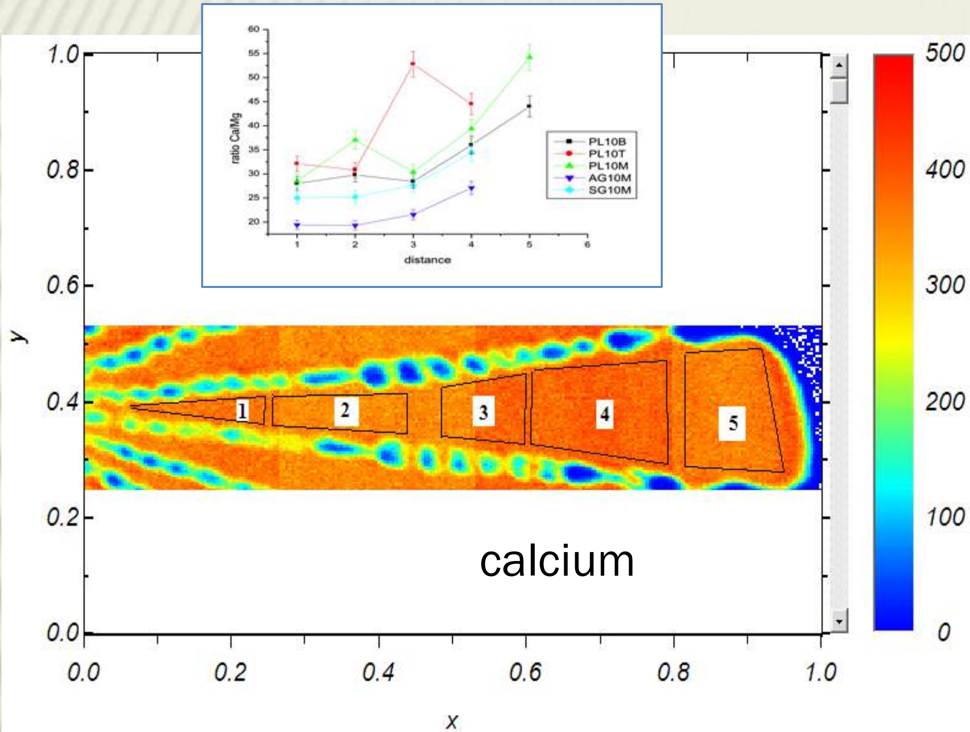

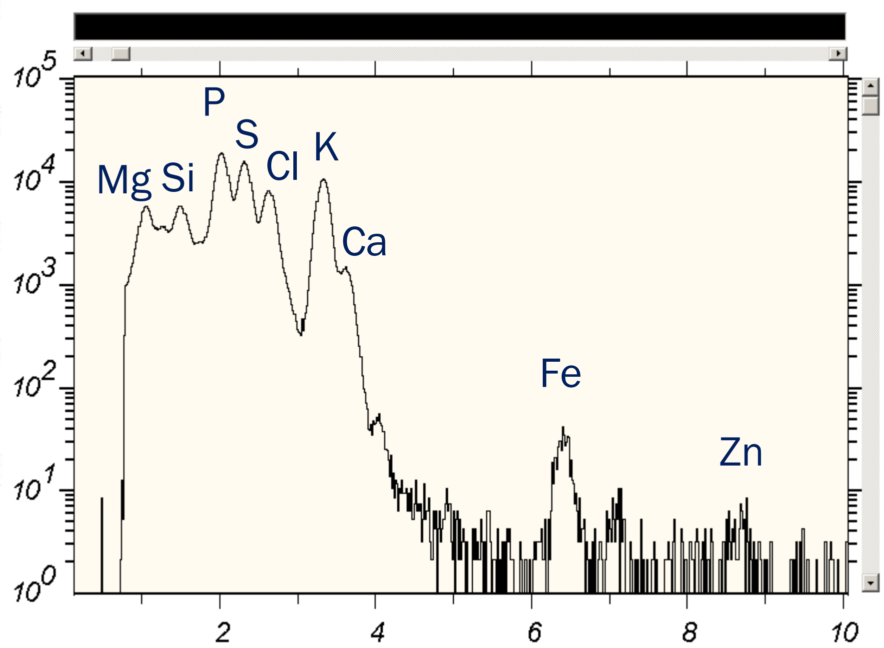

Total Sum	ROI Sum	ROI#	Counts	Cursor
905328	#####	#####	0	10 (0.122522)

Seawater pollution influence on sea-urchin (microbeam PIXE imaging)

NUCLEAR MICROPROBE – PIXE APPLICATIONS

medical

PIXE and STIM maps of a skin section treated with ZnO nanoparticles

Z. Sziksai et al., NIM B 269 (2011) 2278

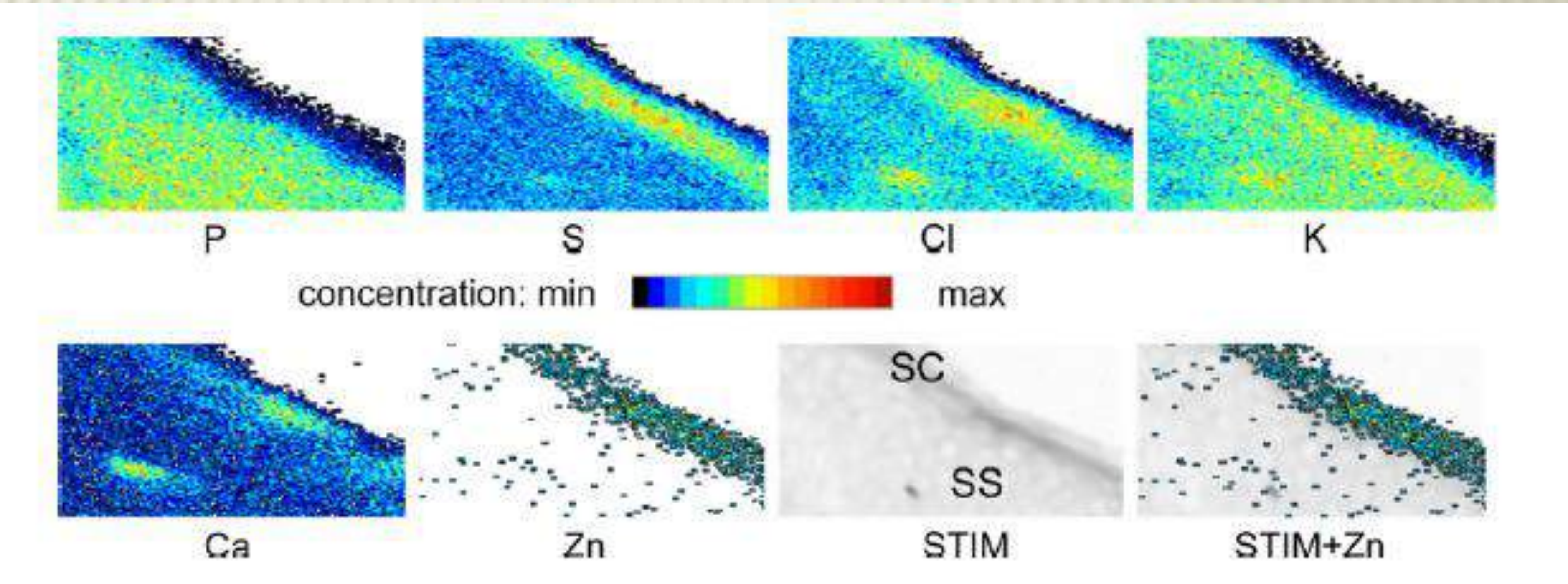

NUCLEAR MICROPROBE – PIXE APPLICATIONS

cultural heritage

Painting by Hans Georg Geiger from the St. Mihael Ch., Gracani

NUCLEAR MICROPROBE – PIXE APPLICATIONS

cultural heritage

2D element distribution of the pigment cross section sample taken from the red area of the painting.

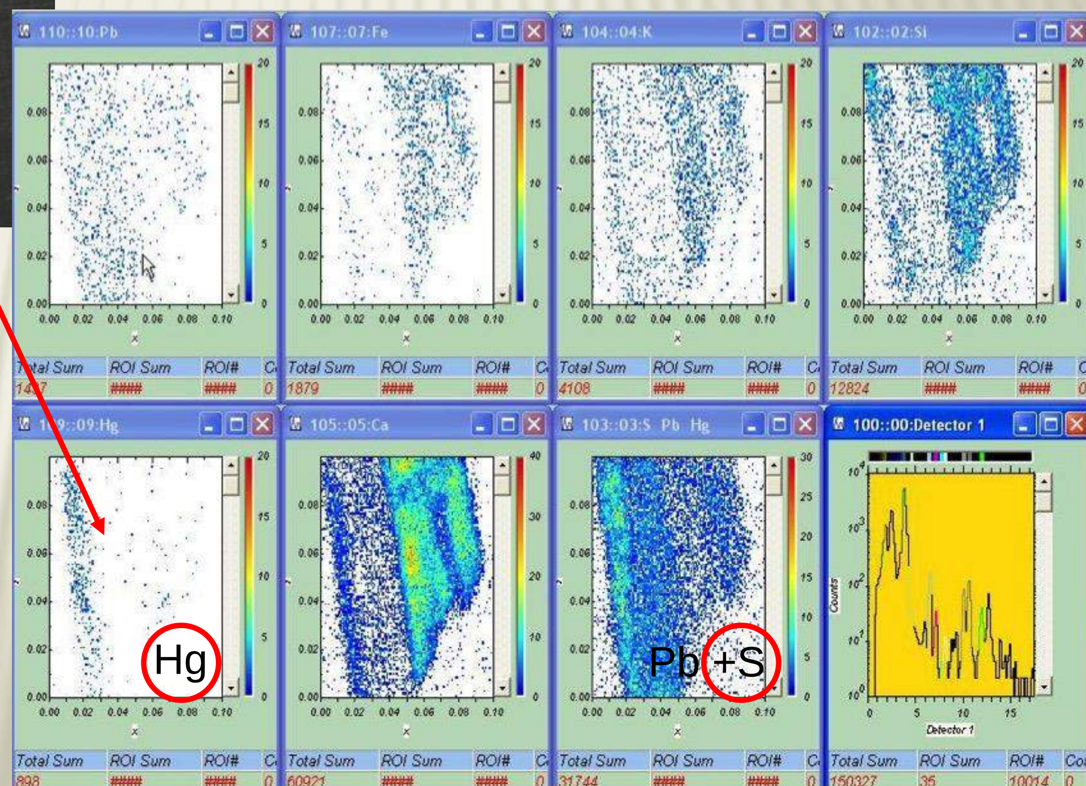

The **light red** layer exhibits high Hg and S concentrations (HgS – cinnabar), while the **dark red** layer beneath shows presence of Pb, Al, Ca,
but without Hg (either minium, or carmine).

OTHER IBA TECHNIQUES

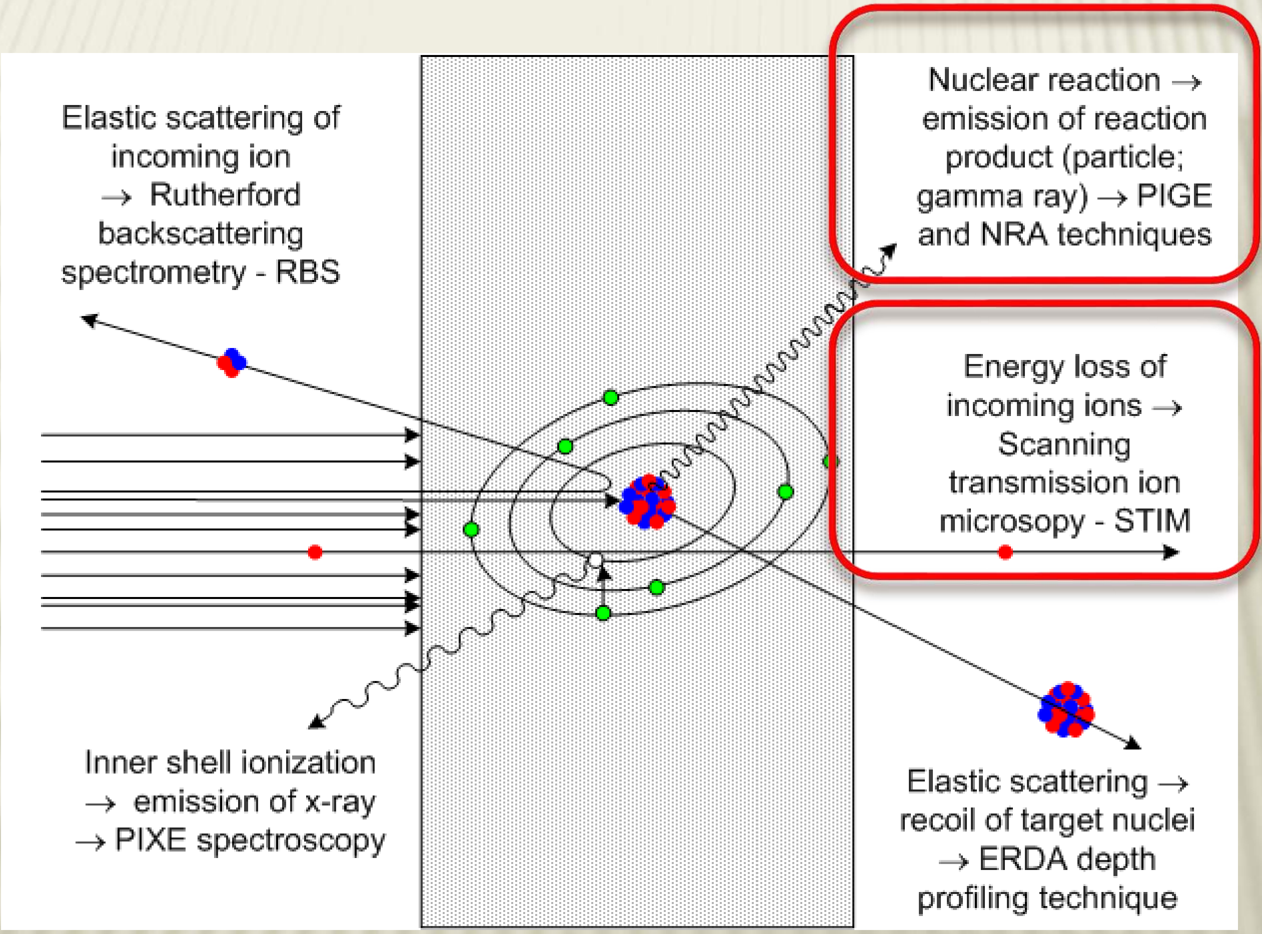

OTHER IBA TECHNIQUES

RBS in channeling (RBS/c)

Secondary electrons SE imaging

Ionolumine scence (IL)

High resolution HR-PIXE

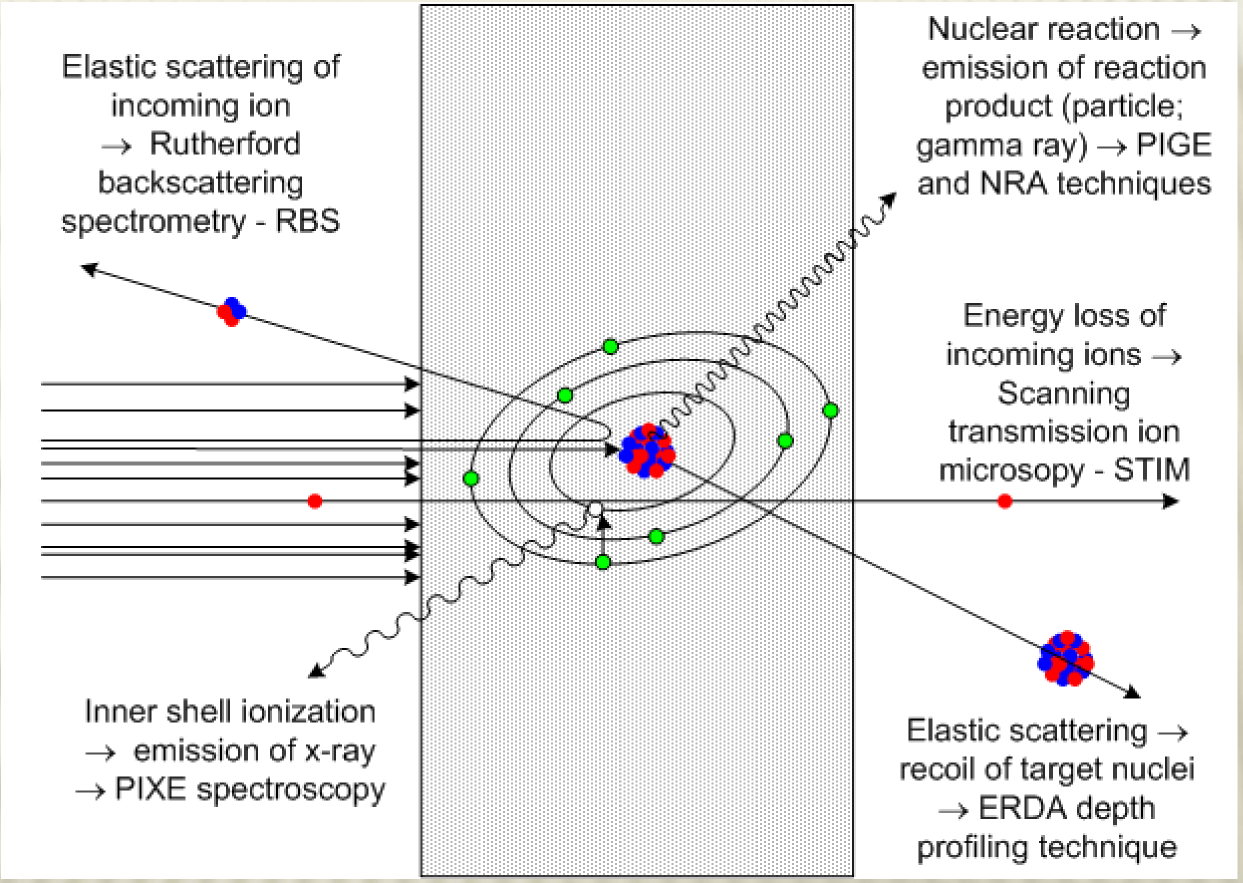

MeV-SIMS

Ion beam induced charge (IBIC)

P-p & C-C scattering

STIM & MeV-SIMS

Ion beam: 9 MeV O^{4+}, image size: 85x85 μm^2 (≈300 nm/pixel)

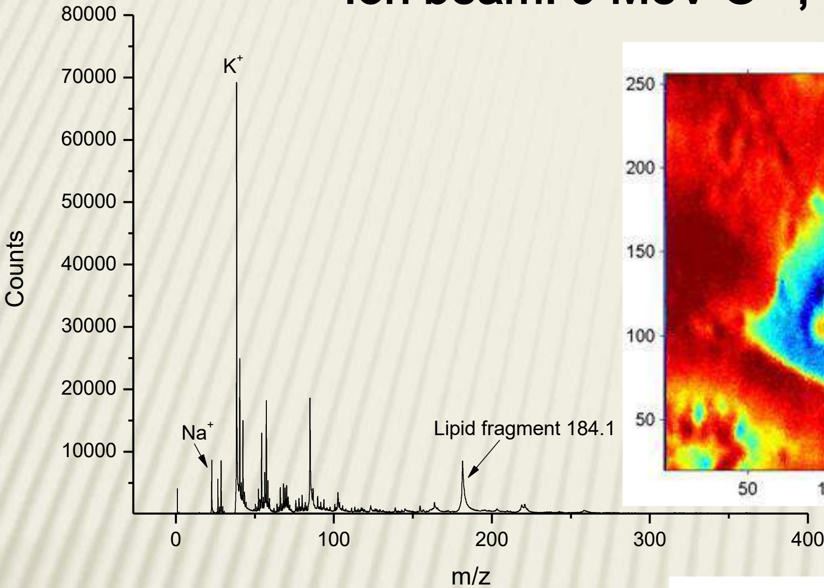

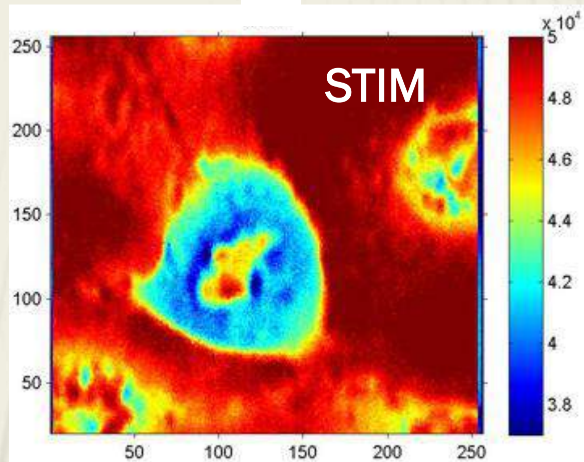

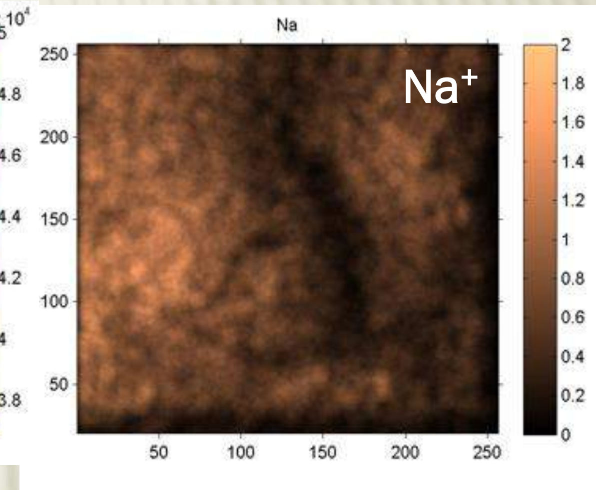

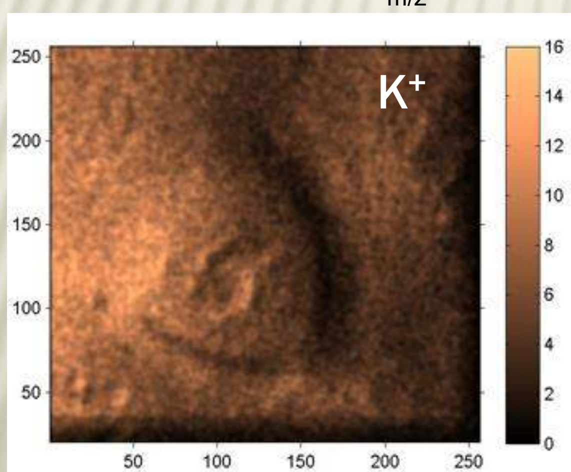

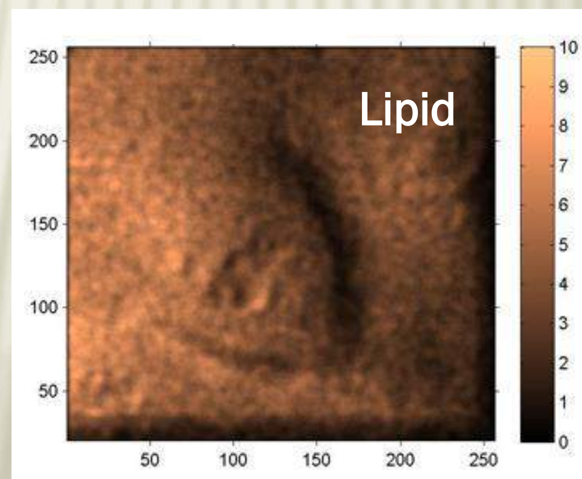

Z. Siketić et al., Appl. Phys. Lett. (2015)

DUAL BEAM FOR *in situ* RBS/C ANALYSIS

5 MeV Si ⇨ SiO_2 quartz
RBS/c: 1 MeV protons

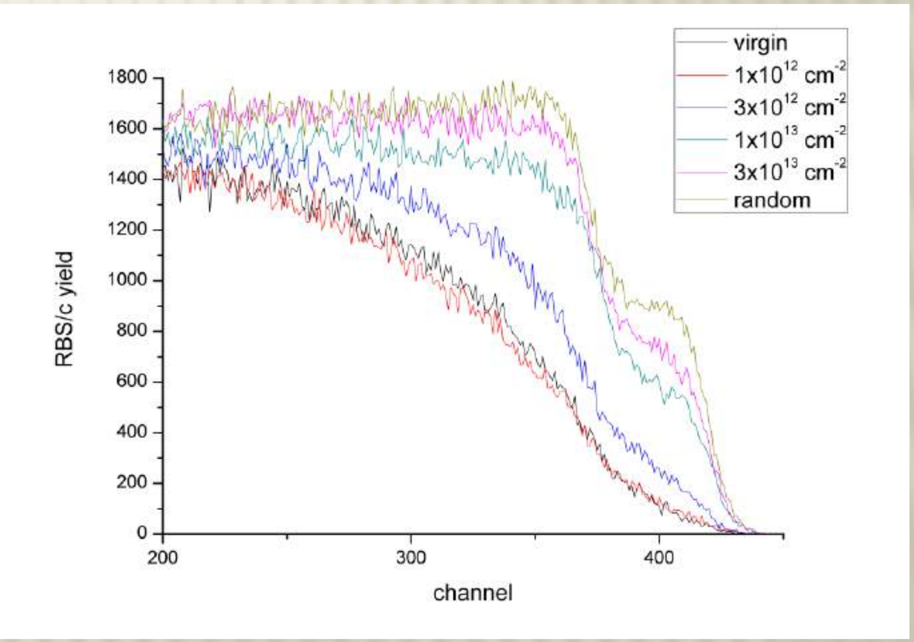

M. Karlušić et al., unpublished

MATERIALS MODIFICATION USING ION BEAMS

Ion implantation:
a) Injection of foreign atoms
b) Displacement of atoms

Single ion tracks:
Fast and heavy ions (~MeV/amu) create latent tracks of damage used as a template in nanostructuring

Irradiation with protons:
Produce homogeneous radiation damage that can be used for lithography, defect engineering, etc..

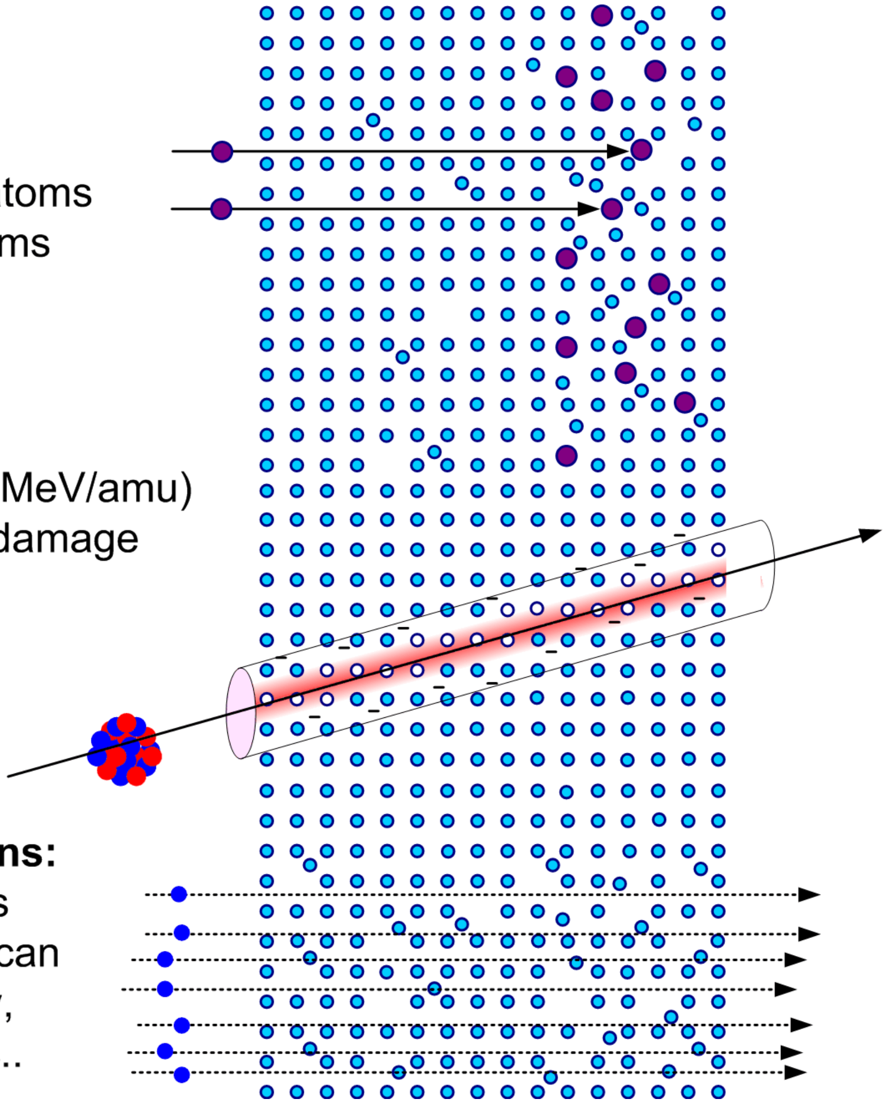

ION ENERGY LOSS

$$-\frac{dE}{dx} = \frac{4\pi n z^2}{m_e v^2} \cdot \left(\frac{e^2}{4\pi\varepsilon_0}\right)^2 \cdot \left[\ln\left(\frac{2m_e v^2}{I}\right)\right].$$

Bethe – Bloch formula

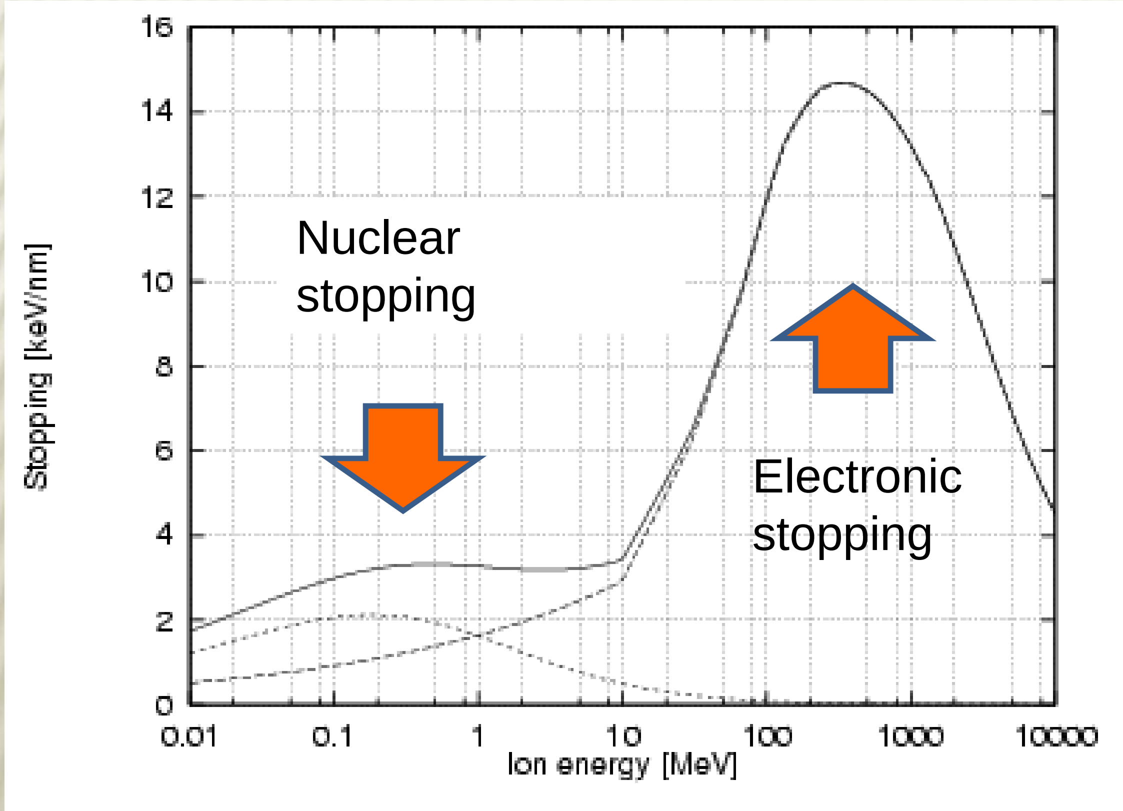

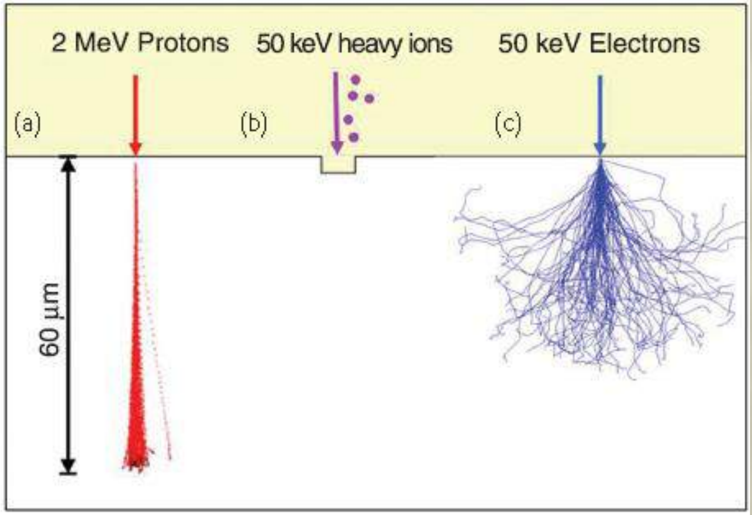

Energy loss of Xe ion in silicon (SRIM)

APPLICATIONS

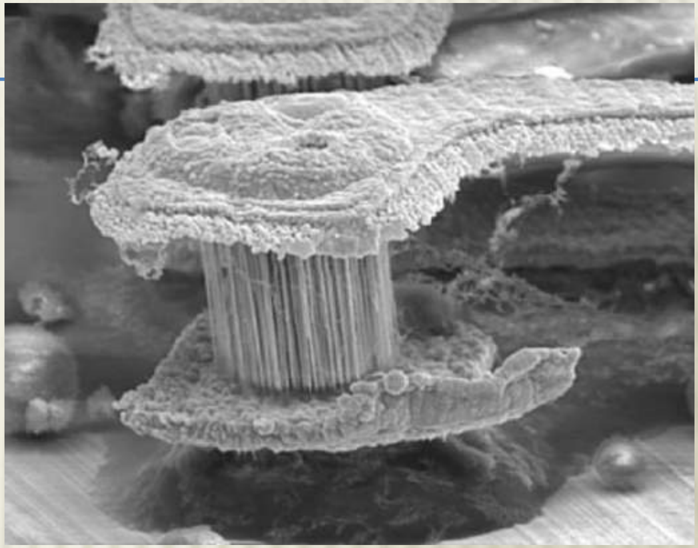

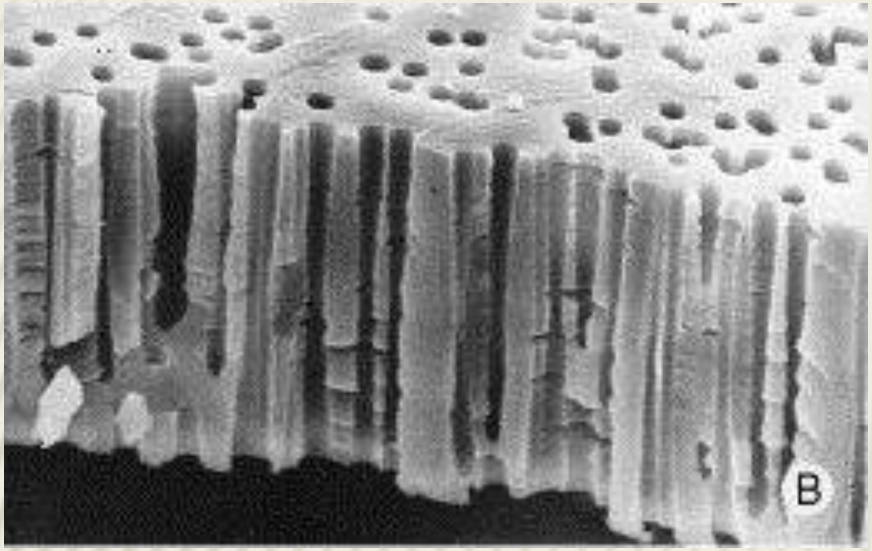

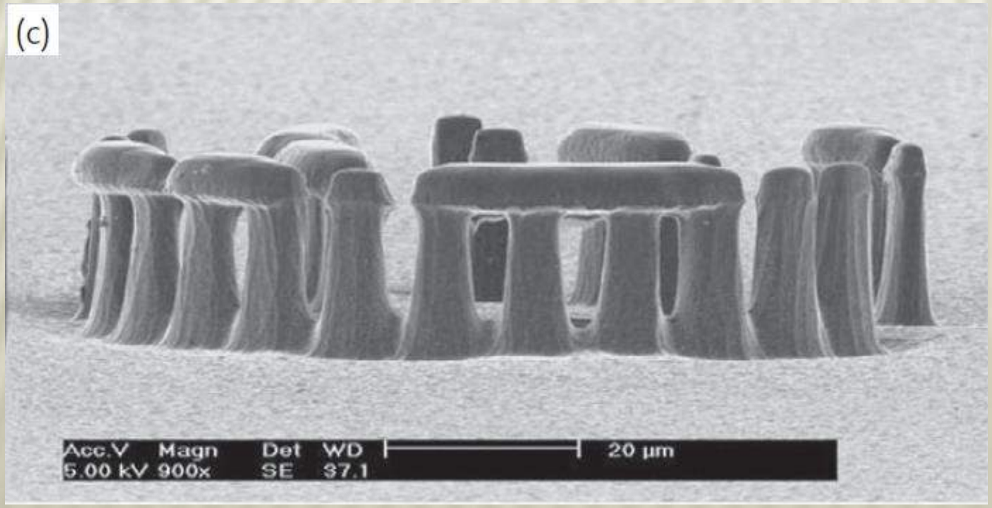

RADIATION DAMAGE IN CAF_2

- Multitechnique approach to analyse nanoscale radiation damage!

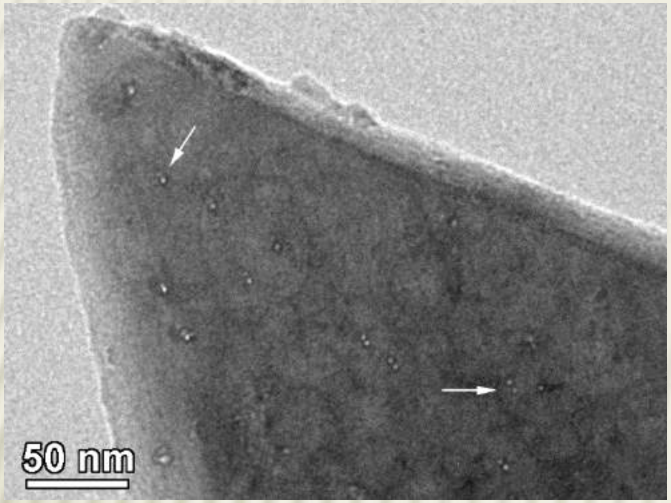

TEM, RBS/c, AFM & ERDA

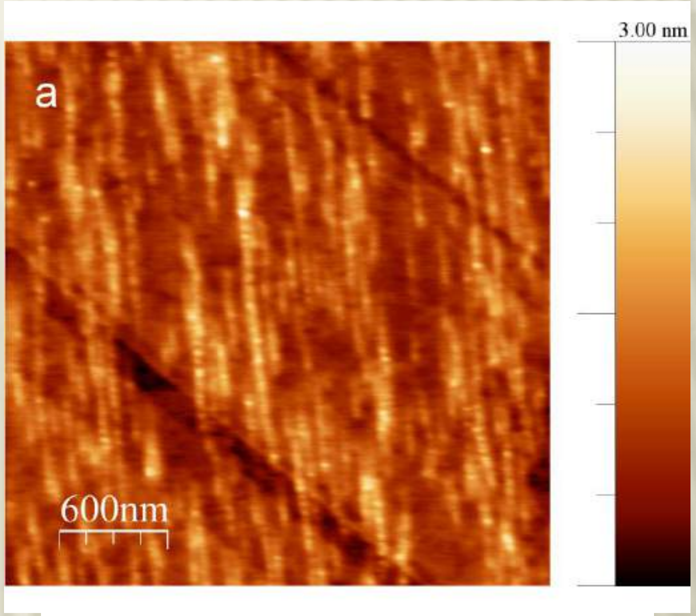

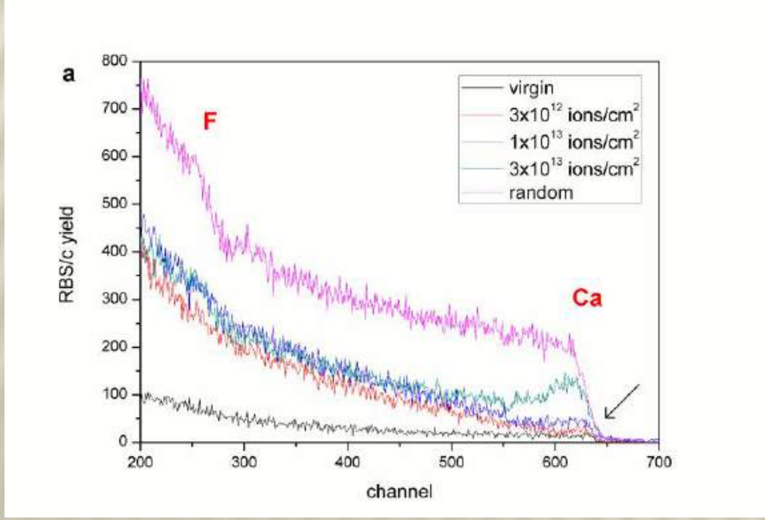

M. Karlušić et al., New J. Phys. (2017)

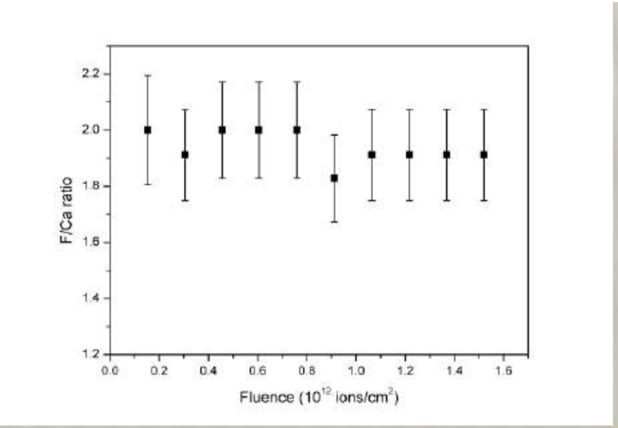

RIPPLES BY GRAZING INCIDENCE SHI

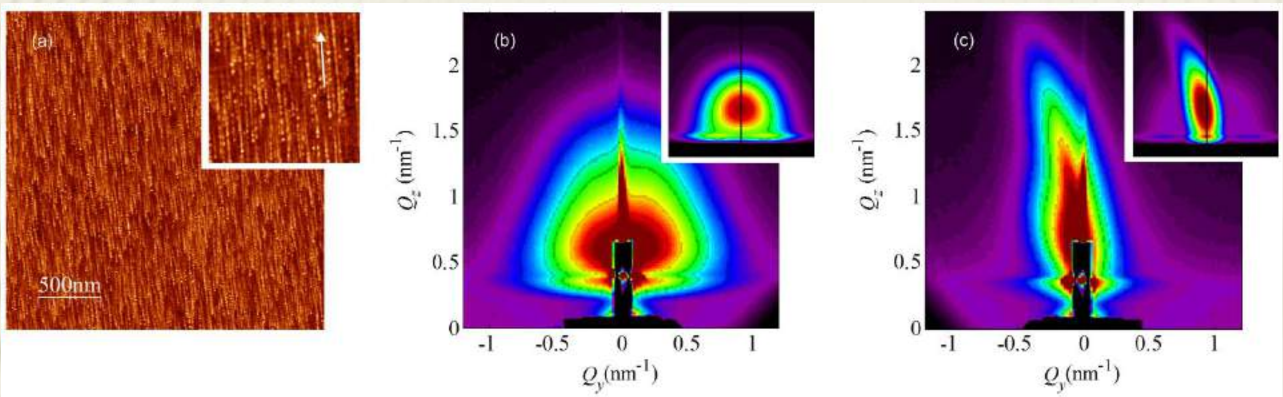

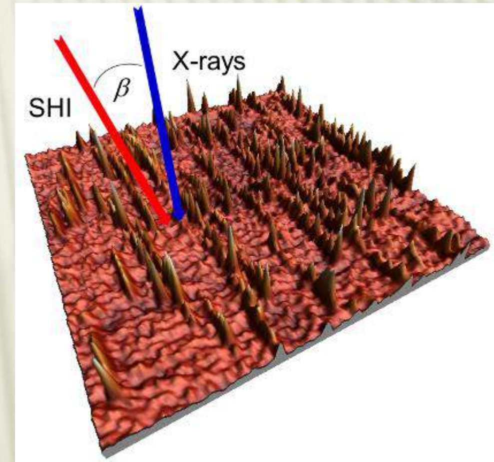

M. Karlušić et al., J. Appl. Cryst. (2016)

AFM & GISAXS

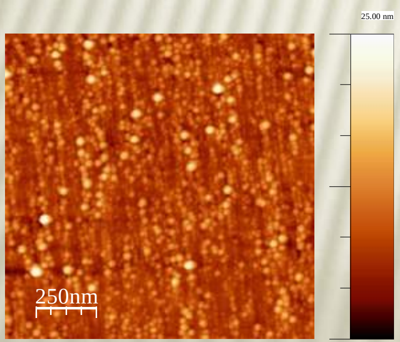

23 MeV I

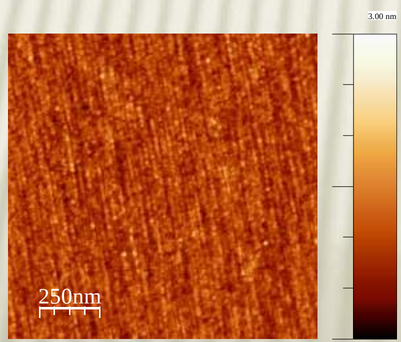

15 MeV Si

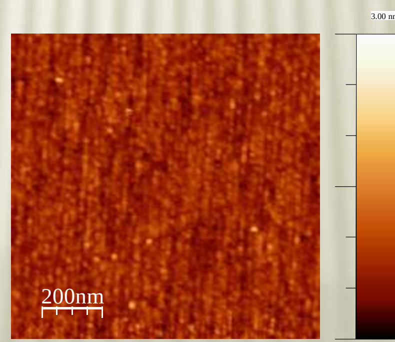

6 MeV Si

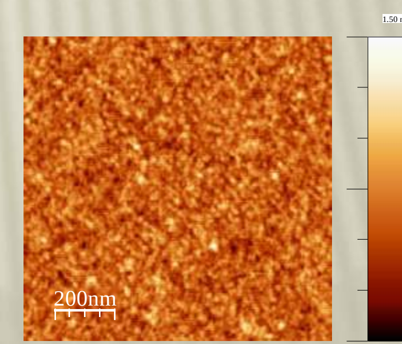

3 MeV O

ION BEAM ASSISTED ORDERING OF QDs

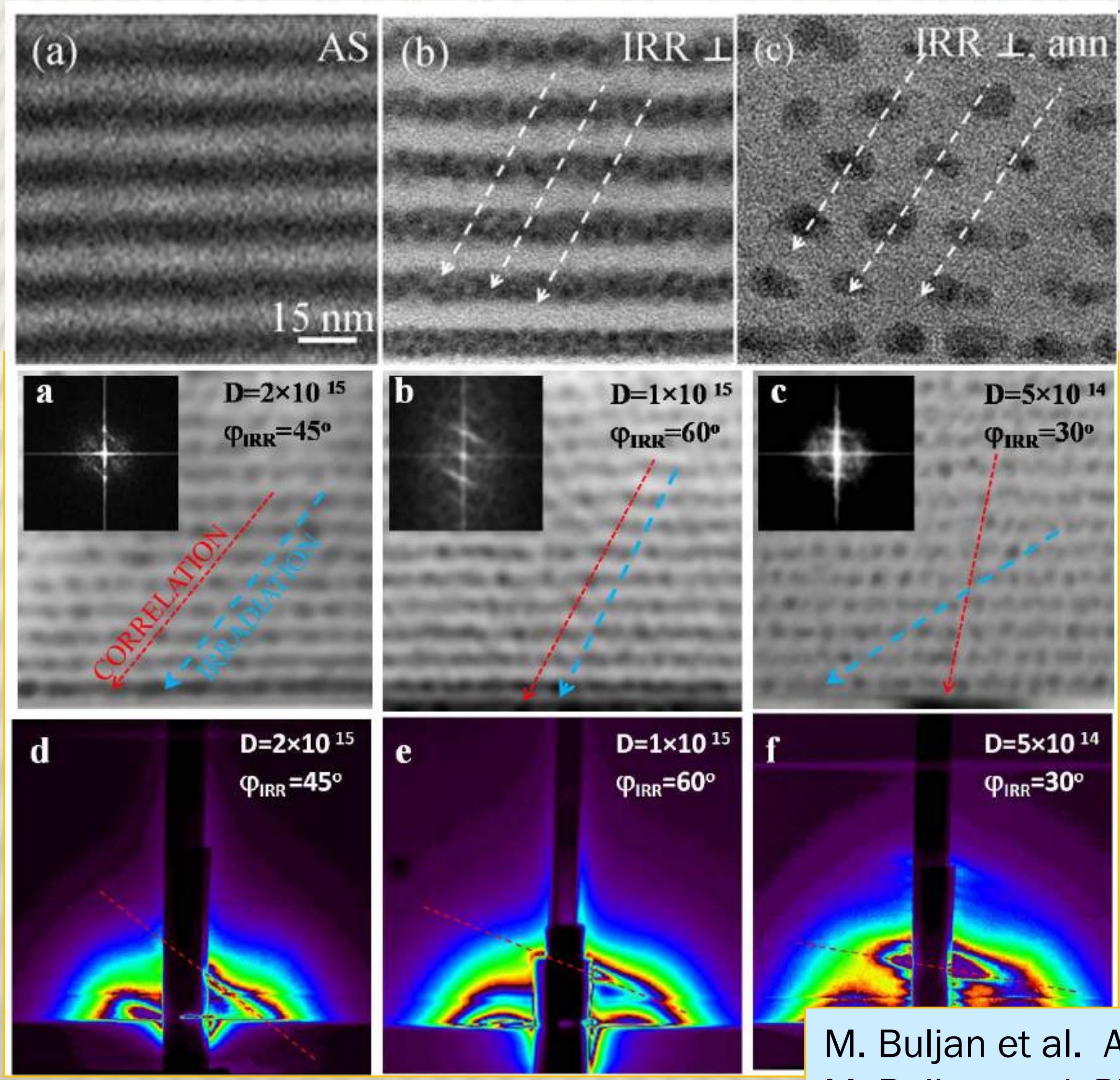

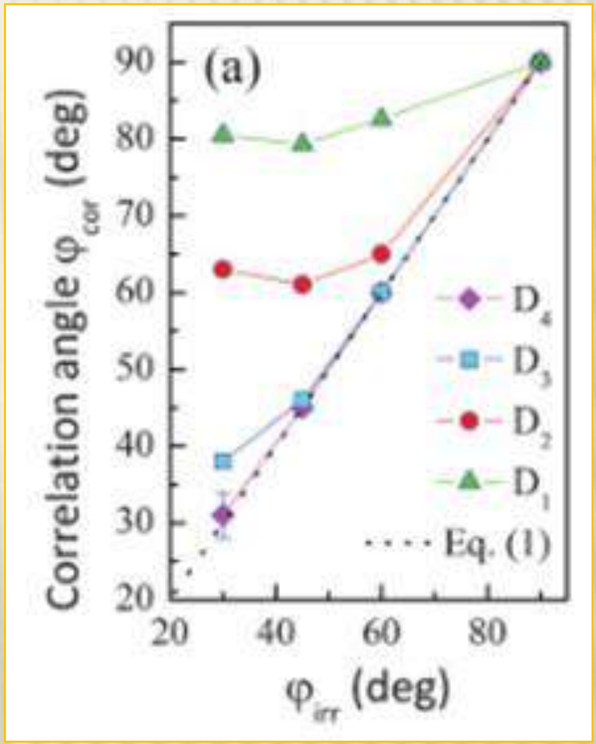

TEM & GISAXS

M. Buljan et al. Appl. Phys. Lett. **95** 063104 (2009).
M. Buljan et al. Phys. Rev. B **81** 085321 (2010).
M. Buljan et al. Phys. Rev. B 84 155312 (2011)

In situ ToF-ERDA ANALYSIS OF ION TRACKS

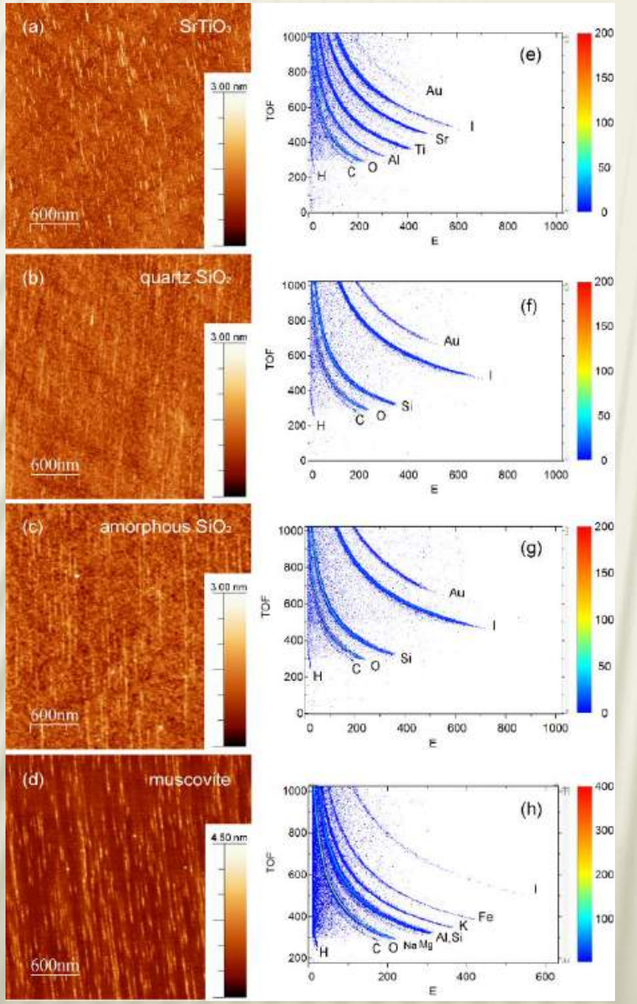

AFM & ERDA

GaN: J. Phys. D: Appl. Phys. (2015)

TiO_2: J. Appl. Cryst. (2016)

CaF_2: New J. Phys. (2017)

PERFORATING GRAPHENE

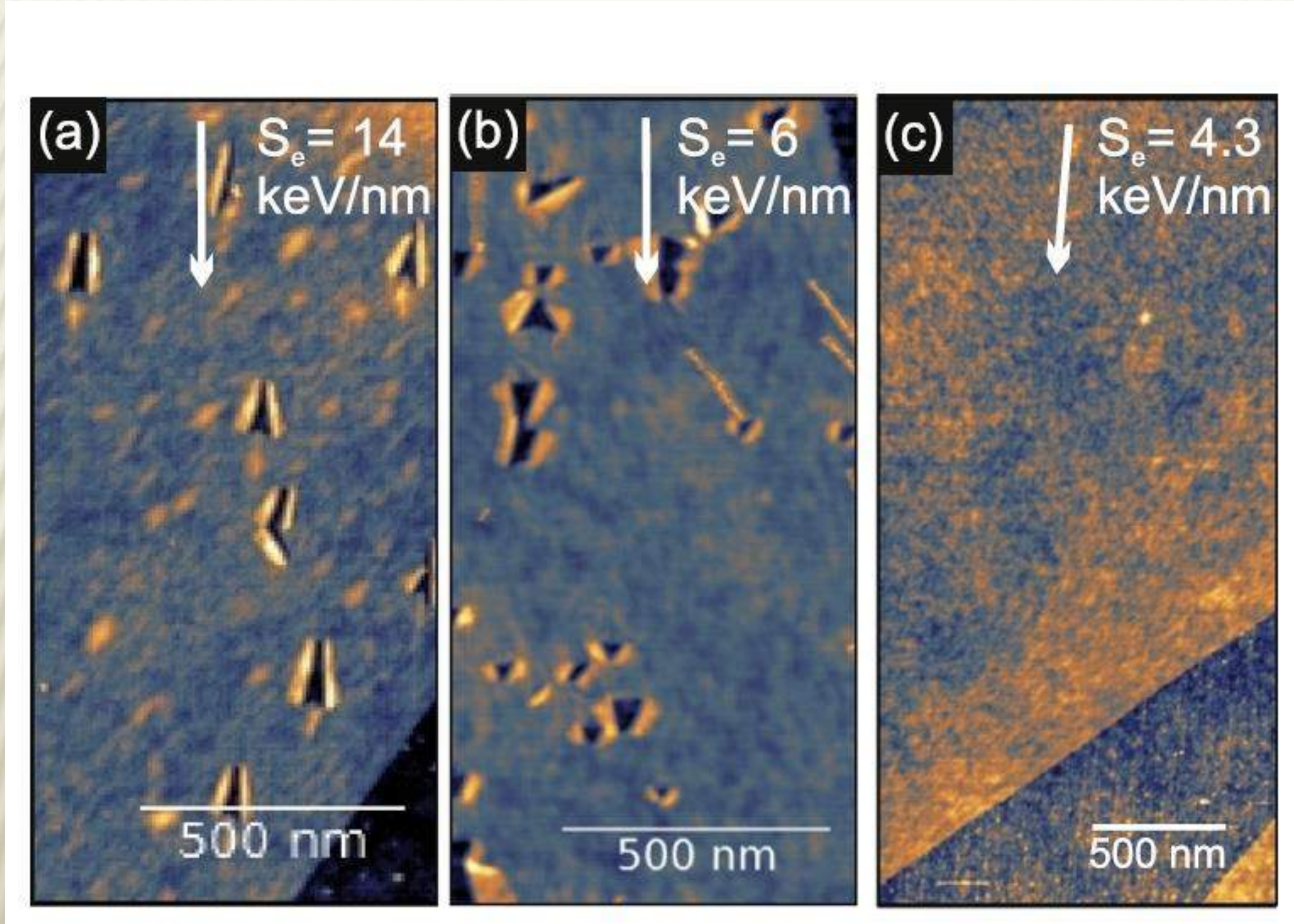

AFM & Raman

O. Ochedowski et al., Nanotechnology (2015)

GANIL
84 MeV Ta

RBI
23 MeV I

15 MeV Si

CONDUCTIVE CHANNELS IN DIAMOND

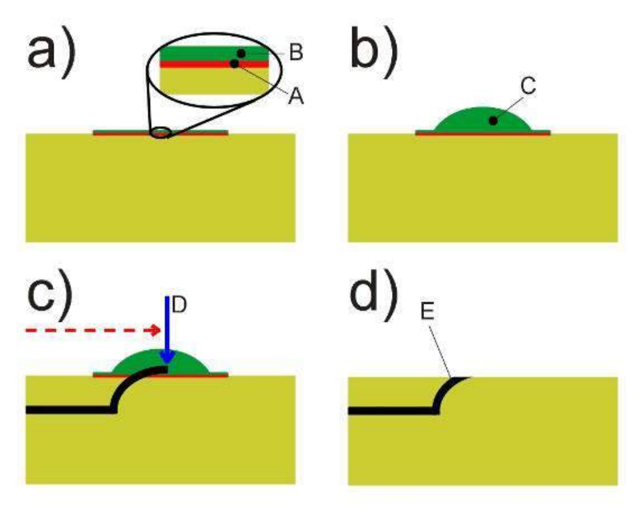

Implantation with three-dimensional masking

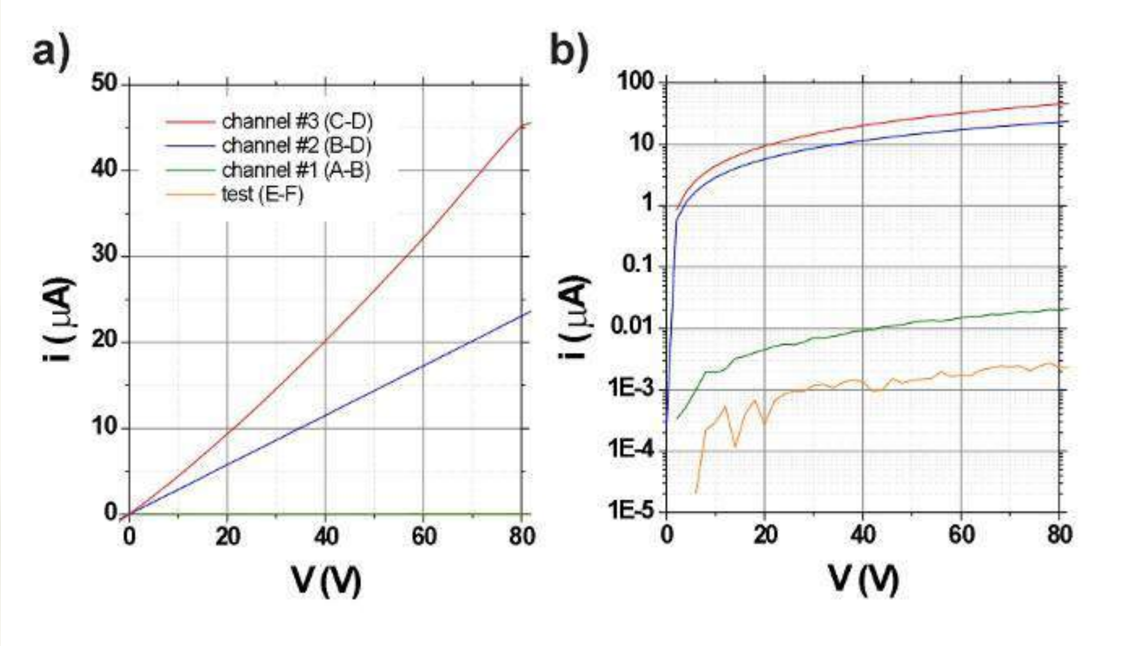

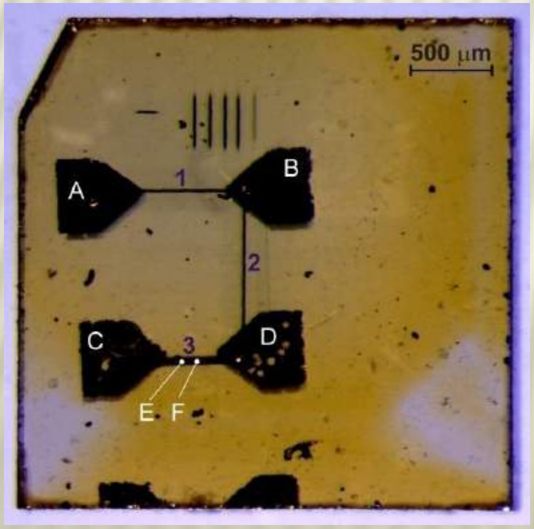

After thermal annealing (900 °C) damaged regions are becoming conductive

Problem: How to make reliable connection?

P. Olivero et al, Diamond Rel. Mat. (2008)

THANK YOU FOR YOUR ATTENTION!

Si pin diode